

0204

DUPLICATE ALSO



Short-range Forecasting Research

Short Range Forecasting Division

Scientific Paper No.5

Radiative Properties of Water and Ice Clouds at Wavelengths Appropriate to the HIRS Instrument Channels

by

A.J. Baran and P.D. Watts

2nd June 1992

**Meteorological Office
London Road
Bracknell
Berkshire
RG12 2SZ
United Kingdom**

ORGS UKMO S
NATIONAL METEOROLOGICAL LIBRARY
FITZROY ROAD, EXETER, DEVON. EX1 3PB

Radiative Properties of Water and Ice Clouds at
Wavelengths Appropriate to the HIRS Instrument
Channels

A.J Baran and P.D Watts

2nd June 1992

Abstract

A detailed theoretical study concerning the infra-red radiative properties of water and ice clouds at wavelengths appropriate to the HIRS (High resolution Infra-red Radiation Sounder) instrument channels is presented. This initial study employs the two-stream approximation for radiative transfer using Mie scattering for a collection of spherical particles to calculate the radiative properties. Future work will calculate bidirectional reflectance. Realistic cloud particle size distributions and concentrations have been used to represent marine stratocumulus, land stratocumulus and cirrus clouds. The results are presented as graphs of the spectral reflection, transmission and emissivity for each of the cloud types across the wavelength range 3.4-15.0 μm . The theoretical results are compared to existing infra-red observations of water and ice clouds. Estimation of water cloud parameters such as optical depth and droplet radius from measurements at 0.7 μm and 3.7 μm respectively is also described.

1 Introduction

Radiative study of water and ice clouds has over the past twenty years become intense. This is because there is a need to understand how a cloud interacts with a radiation field; only with such an understanding can the accuracy of remotely sensed measurements and retrieval of cloud parameters be improved (see for example Hunt (1973), Eyre (1989), Arking and Childs (1985)). A further impetus has come from climate modelling; here it is crucial to understand and quantify the interaction between clouds and radiation as this affects the heating and cooling of the atmosphere (see for example Webster and Stephens (1984) and IPCC report (1990)).

Theoretical study of the interaction of radiation with water clouds has largely been influenced by the work of Yamamoto et al (1970) who calculated the spectral transmittance, reflection and emission of water clouds for the wavelengths between 5-50 μm with a spectral resolution of 50 cm^{-1} . They chose a representative altostratus cloud using the drop size distribution given by Deirmendjian (1969) with the following parameters: particle concentration number 450 cm^{-3} , liquid water content 0.28 gm^{-3} , cloud temperature $-10^{\circ}C$, earth surface temperature $15^{\circ}C$, droplet modal radius 9 μm and total water content 1.44 gm^{-3} . The cloud was assumed to be infinite in horizontal extent with a uniform composition throughout. A modal radius of 9 μm is now known to be large for altostratus; the figure 4.5 μm is often quoted for such a cloud (see for example Paltridge and Platt (1976)). The effect of water vapour absorption in the cloud is taken into account and the angular distribution of scattered radiation is calculated using the real and imaginary parts of the refractive index of water. The full radiative transfer equation including scattering and emission source terms was solved for different cloud thickness using the formulation

of Chandreskhar. The results of the radiative transfer calculations show that for a cloud only 10 m thick the cloud transmittance is considerably less than 1. The emissivity increases with cloud thickness but for an infinitely thick cloud is still less than unity. The cloud spectral reflectance increases with thickness and is greatest at shorter wavelengths; at about $5 \mu m$ it has a value of around 11 %. The spectral reflectance has minima at $6.3 \mu m$ and $12 \mu m$ due to water vapour absorption and refractive index properties of water respectively. The reflectance and emissivity reach their limiting values, to a good approximation, at a cloud depth of 100 m.

Hunt (1973) calculated radiative characteristics of water and ice clouds at 2.3, 3.5, 3.8, 8.5 and $11 \mu m$. Two cloud drop spectra of the type used by Deirmendjian (1969) were employed having modal radii of 4 and $10 \mu m$. For cirrus clouds three size distributions of ice particles were used assuming spheres of modal radii 16, 32 and $50 \mu m$. Water vapour absorption was neglected in the scattering calculations. Hunt found that the infra-red radiative properties of clouds are sensitive to the cloud droplet size. The emissivity of an ice cloud was found to be less than that of a water cloud of the same thickness, due to the decreased water content. A 1 km thick cirrus cloud has an emissivity, according to Hunt's calculations, of about 50 %.

Ridgway and Davies (1983) performed Mie scattering calculations for various cloud types; stratus, stratocumulus and nimbostratus. Representative cloud droplet distributions and modal radii were used although they do not explicitly state the distribution or the values used. Multiple scattering path lengths for reflection and transmission were calculated through Monte Carlo simulations. They modelled water vapour absorption at a resolution of 20 cm^{-1} using Lowtran 5 (Kneizys et al 1980) and the computed reflectance is averaged to 50 cm^{-1} resolution. The spectral reflectance is calculated from

5 to $0.7 \mu m$ for stratus, stratocumulus and nimbostratus with optical depths of 54, 28, 100 respectively, and all 1 km thick. The asymmetry parameter is taken to be 0.86 in each case - a reasonable approximation. They find their highest reflection of 10 % at $4.0 \mu m$ and all their peak reflectances are in water vapour absorption windows and have magnitudes which are governed by the single scattering albedo and optical depth of the clouds. The minima in their reflectance profile is largely due to water vapour absorption above the cloud. At shorter wavelengths the spectral reflectance increases towards unity with increasing optical thickness; this is because the single scattering albedo is close to unity.

Coakley (1991) studied single layered marine stratocumulus and separated the regions into broken and uniform cloud. This was done by using observations collected as part of the First International Satellite Cloud Climatology Project Regional Experiment (FIRE). The reflectivities from the cloud are compared at $0.63 \mu m$ and $3.7 \mu m$. At $0.63 \mu m$ it is found that broken layered cloud reflectivities are lower than that for unbroken layered cloud. At $3.7 \mu m$ it is found to be the other way round. Coakley and Davies (1986) observed the same effect. This effect is attributable to small particles existing at the edge of the broken layered cloud.

The radiation properties of cirrus clouds have been studied by Kuhn and Weickmann (1969) who obtained infra-red transmissivity measurements. For high thin cirrus the transmissivity was found to be 95 % and for cirrus 5 km thick the transmissivity was found to be 53 %. Platt (1973, 1975) found cirrus emissivity, based on observations in the $10-12 \mu m$ region, to be on average 28 %; he also found that the emissivity is more dependent on particle concentration number than cloud thickness. Liou (1974) calculated the infra-red transmission, reflection and emission by means of the Discrete Ordinates

Method for radiative transfer. Cirrus particles were assumed to be long circular cylinders. For a thickness of 1 km and an ice crystal concentration of 0.05 cm^{-3} , the transmittance was found to be about 65 % and emission 35 %. Liou and Coleman (1980), Takano and Liou (1989) have also studied scattering from non-spherical ice crystals. Liu et al (1991) calculated the reflectivities of water and ice clouds for typical particle distributions found in stratocumulus and cirrus cloud types. They found, assuming spherical ice crystals, that thick ice clouds could reflect up to 50 % at a wavelength around $10 \mu\text{m}$. However, the model radius used in this case was about $6 \mu\text{m}$ which is very small for cirrus clouds. Also, their ice crystal concentration number was 1000 cm^{-3} : far too high for cirrus clouds. However, they may have been trying to determine the effects of ice crystals which are not detected by existing microphysical probes.

In the present paper an extensive study of the radiative properties of water and ice clouds is presented for wavelengths in the range $3.4\text{-}15 \mu\text{m}$. This is the wavelength range appropriate to the HIRS instrument channels. Recently obtained physically realistic effective radii and particle concentration numbers are used. Previous papers, as described above, have concentrated on particular wavelengths or a range of wavelengths which has not encompassed all the HIRS instrument channels. This has provided the motivation for the present work. The theoretical results presented are qualitatively compared with the results of previous authors. In addition it is also shown how the optical depth of water clouds, following Arking and Childs (1985), can be estimated from measurements at $0.7 \mu\text{m}$. A method of obtaining the water cloud drop radius from measurements at $3.7 \mu\text{m}$ is also presented; these wavelengths correspond to the HIRS instrument channels 20 and 19 respectively.

2 Mie Scattering

In this paper it is not intended to give a formal treatment of either Mie theory or the two-stream approximation as these are standard and can be found in many text books on electromagnetic theory or radiative transfer (see for example Van de Hulst (1957); Deirmendjian (1969); Lenoble (1985); Liou (1974)). However, the following Mie definitions will help the reader understand the following sections. The single scattering albedo, ω_0 , measures the effectiveness of scattering relative to extinction for radiation incident on a single particle. Probably the most important characteristic of the scattering medium is the phase function, p . This gives the ratio of radiation scattered into a direction to that scattered into the same direction by an isotropic source. More simply the phase function is the angular distribution of scattered radiation. Another important concept used in the following sections is the asymmetry parameter, g , from which the ratio between forward and backscattering can be determined. The scattering cross section is related to the geometric cross section by the efficiency factor, Q . For further details on these concepts the reader is referred to the above references.

3 Cloud Properties and Scattering Calculations

In this paper the radiative properties of marine stratocumulus, land stratocumulus and cirrus clouds are calculated. The stratocumulus clouds are representative of low level water clouds and the cirrus clouds are representative of high level ice clouds. Mie calculations are made for a single spherical particle and we assume that we have a monodispersive collection of particles (monodispersive means a collection of particles with equal radii).

Hunt (1973) assumed a polydisperse collection of particles (meaning a collection of particles with different radii) with a modal radius. However, we use an effective particle radii calculated from the particle droplet spectrum used by Deirmendjian (1969) based on the observed characteristics of water droplet clouds. The distribution function is given by the equation

$$n(r) = ar^6 \exp(-br), \quad (1)$$

where the parameters a and b are given by

$$a = \frac{n}{b^7 6!} \quad (2)$$

and

$$b = \frac{6}{r_c}. \quad (3)$$

In equation (2) n is the particle concentration number in cm^{-3} and r_c is the mode radius of the distribution; $n(r)$ is completely defined given equations (1), (2), (3) and a minimum and maximum particle radius. The particle effective radius, r_{eff} , is defined by the equation

$$r_{eff} = \frac{\int_0^\infty \pi n(r) r^3 dr}{\int_0^\infty \pi n(r) r^2 dr}; \quad (4)$$

r_{eff} is related to the ratio of the total volume to the total surface area of the particles. For the distributions that occur in clouds r_{eff} will always be larger than the modal radius. If in scattering calculations the modal radius is used instead of the effective radius then the cloud reflectance would be overestimated.

The scattering, absorption, extinction coefficients and single scattering albedo for a monodisperse collection of particles with equal effective radii are given respectively by

$$\beta_{sc} = n\pi r^2 Q_{sc},$$

$$\beta_{ab} = n\pi r^2 Q_{ab},$$

$$\beta_{ext} = n\pi r^2 Q_{ext},$$

$$\omega_o = 1 - \frac{\beta_{ab}}{\beta_{ext}}. \quad (5)$$

Table I shows the calculated values for the Mie parameters ω_o and g as calculated by Hunt (1973) and the present author. The calculations in both cases assumed a modified gamma distribution for the droplet spectrum and a particle concentration number 100 cm^{-3} for both water and ice clouds.

Table I. Hunt (1973) and Author Mie Calculations							
cloud	$\lambda \text{ } \mu\text{m}$	Hunt $r_c \text{ } \mu\text{m}$	ω_o	g	Author $r_{eff} \text{ } \mu\text{m}$	ω_o	g
Ice	3.5	16.0	0.592	0.924	18.70	0.587	0.929
Ice	3.5	32.0	0.545	0.953	37.40	0.540	0.955
Ice	11.0	32.0	0.496	0.963	37.40	0.495	0.966
Ice	11.0	16.0	0.524	0.931	18.70	0.508	0.931
Wat	2.3	4.0	0.988	0.801	5.80	0.987	0.800
Wat	2.3	10.0	0.973	0.859	13.45	0.971	0.848
Wat	3.5	10.0	0.728	0.866	13.45	0.701	0.852
Wat	11.0	4.0	0.364	0.849	5.80	0.357	0.841

It is clear from table I that the Mie calculations by Hunt (1973) and the author are in very good agreement.

Mie scattering calculations applied to cirrus clouds are often criticized for assuming spherical ice particles when it is known that cirrus particles are not spherical. They can assume a variety of shapes ranging from hexagonal and needle to star shaped figures. However, Van de Hulst (1957) found that infinite cylinders of circular cross section behave similarly to spherical particles of the same radius. There are numerous data sets supplying

the range of values for stratocumulus. Cirrus is less well documented. There is a belief that many of the small ice crystals are not measured by the existing microphysical probes and that the concentration of these small particles is sufficient to affect the extinction coefficient.

4 Analytic Approximations to the Radiative Transfer Equation

There are a number of approximations to the equation of radiative transfer. Single scattering and two-stream approximations are considered in this paper. The general equation of radiative transfer for a plane-parallel atmosphere, for which the scattering geometry is shown in figure 1, is

$$\mu \frac{dI(\tau; \mu, \phi)}{d\tau} = I(\tau; \mu, \phi) - J(\tau; \mu, \phi) \quad (6)$$

where $\mu = \cos\theta$, τ is the optical depth and ϕ the azimuthal angle. $I(\tau, \mu, \phi)$ is the radiance at a depth τ propagating in direction (μ, ϕ) and $J(\tau, \mu, \phi)$ is the source function of the radiation propagating in direction (μ, ϕ) at a depth τ . The source function may be written as

$$J(\tau; \mu, \phi) = \frac{\omega_o}{4\pi} \int_0^{2\pi} \int_{-1}^1 p(\mu, \phi, \mu', \phi') I(\tau; \mu', \phi') d\mu' d\phi' + J_e(\tau; \mu, \phi) \quad (7)$$

$p(\mu, \phi, \mu', \phi')$ is the phase function and (μ', ϕ') is the scattering direction. $J_e(\tau; \mu, \phi)$ is the external source term which can be written as

$$J_e(\tau; \mu, \phi) = \frac{\omega_o}{4\pi} \pi F_o p(\mu, \phi, -\mu_o, \phi_o) e^{-\frac{\tau}{\mu_o}} \quad (8)$$

The general equation of radiative transfer can be straightforwardly solved for the integrated upward $I^+(\tau; \mu, \phi)$ and downward intensities $I^-(\tau; \mu, \phi)$ for a finite atmosphere

bounded on two sides at $\tau = 0$ and $\tau = \tau_1$ as depicted in figure 2. The solutions for the upward and downward intensities are found to be

$$I^+(\tau; \mu, \phi) = \frac{1}{\mu} \int_{\tau}^{\tau_1} J(t; \mu, \phi) e^{\frac{-(t-\tau)}{\mu}} dt \quad (9)$$

$$I^-(\tau; \mu, \phi) = \frac{1}{\mu} \int_0^{\tau} J(t; \mu, \phi) e^{\frac{-(t-\tau)}{\mu}} dt \quad (10)$$

For the case of single particle scattering the source function is given by

$$J_1(t; \mu, \phi) = \frac{\omega_o}{4\pi} e^{\frac{-(t-\tau)}{\mu}} p(\mu, \phi, \mu_o, \phi_o) \pi F_o \quad (11)$$

Where the subscript 1 denotes single particle scattering. Substituting (11) into (9) one obtains for the reflected intensity

$$I_1^+(\tau = 0) = \frac{\omega_o}{4\pi} p(\mu, \phi, \mu_o, \phi_o) \pi F_o \frac{\mu_o}{\mu + \mu_o} [1 - e^{-\tau_1(\frac{1}{\mu} + \frac{1}{\mu_o})}] \quad (12)$$

The reflection coefficient, $R = [\frac{I_1^+(0)}{\pi \mu_o F_o}]$ is then:

$$R = \frac{\omega_o}{4\pi} p(\mu, \phi, \mu_o, \phi_o) \frac{1}{\mu + \mu_o} [1 - e^{-\tau_1(\frac{1}{\mu} + \frac{1}{\mu_o})}] \quad (13)$$

If in equation (13) $\tau_1 \rightarrow \infty$ then R reduces to

$$R = \frac{\omega_o}{4\pi} \frac{p(\mu, \phi, \mu_o, \phi_o)}{\mu + \mu_o} \quad (14)$$

After a similar analysis for the downward intensity the transmission, $T = [\frac{I_1^-(\tau_1)}{\mu_o \pi F_o}]$ is then:

$$T = \frac{\omega_o}{4\pi} \frac{p(\mu, \phi, \mu_o, \phi_o)}{\mu - \mu_o} [e^{\frac{-\tau_1}{\mu}} - e^{\frac{-\tau_1}{\mu_o}}] \quad (15)$$

If in equation (15) $\tau_1 \rightarrow \infty$ then $T=0$. For clouds with high single scattering albedos multiple scattering will be dominant. Only for clouds with small optical depths and low scattering albedos is the single particle scattering approximation valid.

Normally however, neglecting the multiple scattering term is not justified: the two-stream approximation is another analytic solution of the general equation which includes

the multiple scattering term. The two-stream approximation assumes some functional form for the intensity allowing the radiation field to be split up into two opposing streams $I^+(\tau)$ and $I^-(\tau)$. This allows the general equation to be simplified to two ordinary differential equations which can be solved analytically with appropriate boundary conditions for $I^+(0)$ and $I^-(\tau)$:

$$\begin{aligned}\frac{dI^+(\tau)}{d\tau} &= I^+(\tau)\gamma_1 - I^-(\tau)\gamma_2 - \omega_o\gamma_3\pi F_o e^{-\frac{\tau}{\mu_o}}, \\ \frac{dI^-(\tau)}{d\tau} &= I^+(\tau)\gamma_2 - I^-(\tau)\gamma_1 + \omega_o(1 - \gamma_3)\pi F_o e^{-\frac{\tau}{\mu_o}}.\end{aligned}\quad (16)$$

The functional form of γ_1 , γ_2 , and γ_3 depends on the approximation used; see Meador and Weaver (1980); King and Harshvardhan (1986). This paper follows the approximation of Meador and Weaver (1980) called the 'hybrid modified Eddington-Delta function' which takes into account highly anisotropic phase functions unlike the unmodified and Eddington approximations. In this case

$$\gamma_1 = \frac{7 - 3g^2 - \omega_o(4 + 3g) + \omega_o g^2(4\beta_o + 3g)}{4[1 - g^2(1 - \mu_o)]}\quad (17)$$

$$\gamma_2 = -\frac{1 - g^2 - \omega_o(4 - 3g) - \omega_o g^2(4\beta_o + 3g - 4)}{4[1 - g^2(1 - \mu_o)]}\quad (18)$$

$$\gamma_3 = \beta_o = \frac{1}{2}(1 - \sqrt{3}g\mu_o).$$

The solution for the reflection, $R = \left[\frac{I^+(0)}{\pi\mu_o F_o}\right]$ and the transmission, $T = \left[\frac{I^-(\tau)}{\pi\mu_o F_o}\right]$ for a slab of optical thickness τ (where $\tau = n\sigma_\nu z$: n is the particle concentration number per cm^3 , σ_ν is the scattering cross section for each particle, and z is the cloud depth) is then:

$$\begin{aligned}
R &= \frac{\omega_o}{(1 - \kappa^2 \mu_o^2)[(\kappa + \gamma_1)e^{\kappa\tau} + (\kappa - \gamma_1)e^{-\kappa\tau}]} [(1 - \kappa\mu_o)(\alpha_2 + \kappa\gamma_3)e^{\kappa\tau} \\
&\quad - (1 + \kappa\mu_o)(\alpha_2 - \kappa\gamma_3)e^{-\kappa\tau} - 2\kappa(\gamma_3 - \alpha_2\mu_o)e^{\frac{\tau}{\mu_o}}], \\
T &= e^{-\frac{\tau}{\mu_o}} \left(1 - \frac{\omega_o}{(1 - \kappa^2 \mu_o^2)[(\kappa + \gamma_1)e^{\kappa\tau} + (\kappa - \gamma_1)e^{-\kappa\tau}]} \right. \\
&\quad \times [(1 + \kappa\mu_o)(\alpha_1 + \kappa\gamma_4)e^{\kappa\tau} \\
&\quad \left. - (1 - \kappa\mu_o)(\alpha_1 - \kappa\gamma_4)e^{-\kappa\tau} - 2\kappa(\gamma_4 + \alpha_1\mu_o)e^{\frac{\tau}{\mu_o}}] \right). \tag{19}
\end{aligned}$$

If in equation (19) $\tau \rightarrow \infty$ then R reduces to

$$R = \frac{\omega_o(\alpha_2 + \kappa\gamma_3)}{(1 + \kappa\mu_o)(\kappa + \gamma_1)}. \tag{20}$$

γ_4 , α_1 , α_2 , and κ are given by the relations

$$\begin{aligned}
\gamma_4 &= 1 - \gamma_3, \\
\alpha_1 &= \gamma_1\gamma_4 + \gamma_2\gamma_3, \\
\alpha_2 &= \gamma_1\gamma_3 + \gamma_2\gamma_4, \\
\kappa &= \sqrt{(\gamma_1^2 - \gamma_2^2)}. \tag{21}
\end{aligned}$$

The two-stream method can be extended to N streams for greater accuracy. For a more complete treatment the reader is referred to Liou (1974). The two-stream method has been compared by Liou (1974) to the Discrete Ordinate Method and was found to have an accuracy of 10 % in most cases. For this work the two-stream approximation is deemed accurate enough.

5 Two-Stream Model Test

This section is concerned with testing the two-stream calculations against those of other authors. In the calculations that follow the Mie coefficients are calculated from the refractive indices of water and ice, values for which have been taken from Irvine and Pollack (1968) and Warren (1984) respectively and are shown in figure 3 as a function of wavelength. The real and imaginary parts of the refractive index are the fundamental parameters determining the scattering and absorption of the incident wavelength. Figure 4 show the coefficients of absorption and scattering in units of cm^{-1} for a typical small cloud drop. For wavelengths less than $1.5 \mu m$ the imaginary part of the refractive index of water is small and the drop is almost completely scattering. At 3 and $6 \mu m$ the absorption coefficient exhibits large maxima and the gap between 7 and $9 \mu m$ corresponds to the window of transparency in the liquid water spectrum. For wavelengths just greater than $11 \mu m$ the absorption coefficient is greater than the scattering coefficient. This means that the amount of radiation being absorbed by a typical cloud droplet is greater than that being scattered.

Figure 5 shows a comparison between a reflection pattern calculated by Dr. J. Foot (private communication), using the formulation of Chandreskhar, and the author, using both the two-stream and single scattering approximations, for a semi infinite cloud. As can be seen from figure 5 the agreement between the Chandreskhar and two-stream calculations is very good and the two-stream approximation is just within the quoted accuracy of 10 %. The reflection pattern is also in good agreement with other authors such as Shifrin (1961), Yamamoto et al (1971), Ridgway and Davies (1986), and Liu et al (1991). However, the single particle scattering calculations are in poor agreement showing that in

the case of an infinite water cloud multiple scattering predominates. The peak reflectance in the single particle scattering case occurs at $5 \mu m$ which corresponds to the minima in the extinction coefficient in figure 6. The absorption coefficient is shown in figure 7 and becomes large after $5 \mu m$.

6 Results

In the graphs that follow. The radiative properties of water and ice clouds have been calculated using equations (19) and (22) and complete results are given in figures (8-16) for the readers reference. By conservation of energy, at any wavelength the sum of the hemisphere-averaged reflection (r), transmission (t) and emission (ϵ) as given by equation (22) is unity.

$$t + \epsilon + r = 1. \quad (22)$$

The following cases have been chosen; marine and land stratocumulus and ice clouds. The particle effective radius and cloud particle concentration number used in the present calculations were obtained from the recent FIRE and ICE experiments (see for example I.C.E./EUREX report 1991, Albrecht (1989), and Cooper (1989)). The microphysical cloud parameters, r_{eff} , n and cloud depth z adopted are as follows.

(i) Marine Stratocumulus

$$r_{eff} = 10 - 15 \mu m$$

$$n = 50 - 200 cm^{-3}$$

$$z = 100 - 500 m$$

(ii) Land Stratocumulus

$$r_{eff} = 5 - 10 \mu m$$

$$n \leq 400 cm^{-3}$$

$$z = 100 - 500 m$$

(iii) Cirrus

$$r_{eff} = 18 - 40 \mu m$$

$$n = 0.01 - 0.1 cm^{-3}$$

$$z = 100 - 3000 m$$

The number densities, effective radii, solar zenith value and cloud depths are given on each of the graphs and the transmission, emission and reflection profiles are marked T, E and R.

6.1 Water Clouds

In general the positions of the maxima and minima at $3.83 \mu m$ and $6.05 \mu m$ and the broad maxima between $6-10 \mu m$ in the reflection and transmission profiles (figures 8-13) do not change position when varying the particle effective radii; they depend principally on the refractive index of water. For marine and land stratocumulus the radiative calculations show that thin stratocumulus with small drop sizes are transmissive but the transmittance decreases sharply for cloud thickness over 100 m in agreement with Yamamoto et al (1970).

However, very thin stratocumulus does occur and these calculations show that for this case the assumption of a zero transmittance should not be made. At a thickness of 300 m the transmittance is negligible. (Figures 9-10) show the values of the reflectivity vary according to the effective radius and to a much lesser extent the particle concentration number. For a small effective radius, in the case of land stratocumulus, reflectivities can be very high: up to 42 % for a solar zenith value 0.5. Even at wavelengths of 4.0 and 5.0 μm the reflectivities can be 30 and 20 % . The reflection between 6-10 μm is slowly varying, this is due to the slowly varying refractive index of water between these wavelengths. Between 10-15 μm the reflectance slowly increases but only has values ranging from 1-3 %. The conclusion to be drawn from this is that for land stratocumulus with the smaller effective radii the reflectivities are significant and would appear to be so for all the shortwave HIRS channels. For the same wavelength range (channels 13-17), marine stratocumulus and an overhead sun, the reflectivities range from 10-5 %, which is less significant. Larger particles are more efficient absorbers and the high sun means less forward scattering. For a low level solar zenith value the higher reflectivity is due to a component of the forward scattering contributing to the hemispheric reflectance - the HIRS instrument geometry mean that such large reflectances may not be observed.

In summary, the reflection profiles for land stratocumulus are more significant than for marine stratocumulus. This is a result of high particle concentrations and small radii. However, the reflectivities of marine stratocumulus is not insubstantial.

6.2 Ice Clouds

The radiative properties for cirrus clouds are shown in figures (14-16) for a solar zenith value 0.5 and 1.0. The main differences between the cirrus and stratocumulus clouds is the particle concentration number and particle effective radii. For cirrus clouds with depths of a 100 m and relatively large effective radii, $37 \mu m$, the cloud is highly transmitting: $T=95 \%$. As the cirrus cloud thickens to 3 km, maxima of around 6 and 5 % appear in the reflection profile at 3.8 and $5.2 \mu m$. The transmittances also have maxima of about 32 and 26 % at these wavelengths and the emissivity corresponding minima. Between 6 and $11 \mu m$ the refractive index of ice is slowly varying. As the thickness of the cloud increases from 100 m to 3 km the amplitudes of the maxima and minima increase but remain at the same positions. This is the case even as the effective radii and particle concentration number change; as in the water cloud case these positions are determined by the refractive index. The reflection from cirrus clouds is in general small, this is due to the large effective radii and small particle concentrations found in cirrus clouds. These radiative characteristics are in broad agreement with Kuhn and Weickmann (1969) for thin high cirrus clouds, Liou (1974) for $8-12 \mu m$ and Liu et al (1991).

Comparing the water and ice cloud spectral profiles reveals that the peaks in the cirrus reflections are slightly shifted compared to the reflection peaks in the water cloud case. Also, the cirrus emission profile between $8-10 \mu m$ is a sinc function which is pronounced for deep cirrus; such a feature is not present in the water cloud case. These salient differences could be used as a means of identifying cirrus. Cirrus have much lower reflectivities and are greyer, however the cloud is higher, because of lower atmospheric transmittance, can still reflect significantly

7 Water Cloud Parameter Estimation

Arking and Childs (1985) showed how it was possible to retrieve several cloud parameters from satellite radiance measurements. In particular they demonstrated a method for estimating the cloud optical depth from measurements at $0.7 \mu m$ and droplet radius from measurements at $3.7 \mu m$. This paper gives a somewhat different method of estimating the droplet radius to the method of Arking and Childs (1985). Figure 17 shows that at a wavelength of $0.7 \mu m$ the reflectivity depends weakly on the effective radius for a fixed optical depth. Conversely Figure 18 shows a very strong dependence of $0.7 \mu m$ reflectance on optical depth for a fixed effective radius. The reflectance at first rises quickly with increasing optical depth until a monotonic value is reached by an optical depth of about 30. This is in agreement with Arking and Childs (1985), Twomey and Sefton (1980) and Rawlins and Foot (1990) who suggested that at visible wavelengths the reflectivity is independent of effective radius but dependent on optical depth. Therefore, it should be possible to estimate the optical depth from measurements at a wavelength of $0.7 \mu m$. This is the wavelength of the HIRS instrument channel 20.

Figure 19 shows the reflectance at $3.75 \mu m$ for increasing drop radius and particle concentration number $250 cm^{-3}$. Reflectances calculated using the two-stream approximation are indicated by the asterisk signs; the crosses are cloud drop radii estimated from the reflectance measured at $3.7 \mu m$ using the fitted equation

$$r = \frac{|\ln R|}{\gamma} - 0.0002, \quad (23)$$

where $\gamma = 16.9$. It can be seen from figure 19 that the fit is very good. Equation (23) could be used to estimate the cloud drop radius for a water cloud although the accuracy at higher radii would be lower than for low drop radius. However, its direct application may

be limited as it does not take into account any bidirectional properties of the reflectance. Figure 20 shows for three particle sizes the logarithm of the scattered intensity of an incident wave at 3.75 on a particle μm from 0 to 360 degrees. The figure clearly shows the changing intensity pattern for different sized particles and suggests that for estimating a droplet radius the bidirectional reflectance and drop size dependence both need to be taken into account.

Conclusion

The radiative properties of water and ice clouds in the infra-red region 3.4-15 μm have been calculated for typical marine stratocumulus, land stratocumulus and cirrus. This wavelength range is appropriate to the HIRS instrument channels. The calculations show that thin marine and land stratocumulus are highly transmitting and have resulting low reflectivities. Increasing the cloud thickness dramatically reduces the transmission to almost zero. The amount of radiation reflected is chiefly dependent upon the cloud particle effective radius. There is also a dependence on the solar zenith angle. The peaks and troughs in the radiative profiles do not depend upon effective radii but on the refractive index. Clearly, the reflectances from stratocumulus clouds are not insignificant this may have important implications in the interpretation of HIRS channel data.

The calculations have shown that for cirrus clouds the reflectivity is not zero, even for the thinnest clouds. For thick cirrus the reflectivity at 3.8 μm can reach 6 – 8 %, for a solar zenith value 0.5. In general the transmittances for cirrus cloud are dominant but for the thickest cirrus clouds (depths about 3 km) these are substantially reduced for the clouds with the larger effective radii.

It has been shown that it should be possible, using measurements at 0.7 μm and 3.7 μm , respectively, to estimate the water cloud parameters optical depth and cloud drop radius. However, the bidirectional properties of reflectance will almost certainly need to be taken into account and is the subject of current research.

Acknowledgements

The authors wish to express their thanks to Dr. A. Gadd for allowing this work to be done and Dr. J. Foot for helpful comments regarding the manuscript.

References

1. Albrecht A: 1989. Symposium on the role of clouds in atmospheric chemistry and global climate pgs 9-13.
2. Arking A and Childs J.D: 1985. Retrieval of cloud parameters from multispectral satellite images. *J.Climate and App.Met.* Vol 24 No 4 pgs 322-333.
3. Carrier L.W, Cato G.A and Von Essen K.J: 1967. The backscattering and extinction of visible and infra-red radiation by selected major cloud models. *Appl.Opt.* Vol 6, pgs 1209-1216.
4. Coakley J.A and Davies R: 1986. The effect of cloud sides on reflected solar radiation as deduced from satellite observations. *J.Atmos.Sci.* Vol 43 pgs 1025 -1035.
5. Coakley J.A: 1991. Reflectivities of uniform and broken layered cloud. *Tellus* 43B. pgs 420-433.
6. Cooper A: 1989. Symposium on the role of clouds in atmospheric chemistry and global climate pgs 316-318.
7. Deirmendjian D: 1969. *Electromagnetic scattering on spherical polydispersions.* Elsevier. New York.
8. Eyre J.R and Watts P.D: 1987. A sequential estimation approach to cloud- clearing

for satellite temperature soundings. *Quart.J.R.Met.Soc*, Vol 113, pgs 1349-1376.

9. Eyre J.R: 1989. Inversion of cloudy satellite soundings radiances by non-linear optimal estimation II: Application of TOVS data. *Quart.J.R.Met.Soc*, Vol 115, pgs 1027-1038.

10. Foot.J. Private Communication.

11. Goody R.M and Yung Y.L: 1989. Atmospheric radiation theoretical basis. Oxford University Press, Oxford.

12. Hunt G.E: 1973. Radiative properties of terrestrial clouds at visible and infra-red thermal window wavelengths. *Quart.J.R.Met.Soc*. Vol 19, pgs 346-369.

13. I.C.E/EUREX (1991). Report of the fourth workshop, Reading U.K 1-3 July 1991.

14. IPCC Report (1990).

15. Irvine W.M and Pollack J.B: 1968. Infrad-Red optical properties of water and ice spheres. *Icarus*, Vol 8, pgs 324-360.

16. King M.D and Harshvardhan: 1986. Comparative accuracy of selected multiple scattering approximations. *J.Atmos.Sci*. Vol 43, No 8, pgs 784-801.

17. Kneizys F.X, Shettle W.D, Gallery J.H, Chetwynd Jr L.W, Aveu J.E.A, Selby R.W, Mcclatchey R.A: 1980. Atmospheric transmittance/radiance: computer code: Lowtran 5. AFGL-TR-80-0067. Air Force Geophysical Lab Bedford, Mass.

18. Kuhn P.M and Weickmann H.K: 1969. High altitude radiometric measurements

of cirrus. *J.Appl.Meteor.* Vol 8, pgs 147-154.

19. Lenoble J: 1985. Radiative transfer in scattering and absorbing atmospheres: Standard computational procedures. A. Deepak publishing.

20. Liou K.N: 1974. On the radiative properties of cirrus in the window region and their influence on the remote sensing of the atmosphere. *J.Atmos.Sci.* Vol 31, pgs 522-532.

21. Liou K.N: 1974. Analytic two-stream and four-stream solutions for radiative transfer. *J.Atmos.Sci.* Vol 31, pgs 473-1475.

22. Liou K.N and Coleman R.F: 1980. Light scattering by hexagonal columns and plates. pg 207. Light scattering by irregularly shaped particles. Edited by D.W Schuerman, Plenum Press. New York and London.

23. Liu Q. Simmer C. and Ruprech.E: 1991. A general analytic expression for the radiation source function of emitting and scattering media within the matrix operator method. *Beitr.Phy.Atmosph.* Vol 64, No 2, pgs 73-82.

24. Meador W.E and Weaver W.R: 1980. Two-stream approximations to radiative transfer in planetary atmospheres: A unified description of existing methods and a new improvement. *J.Atmos.Sci.* Vol 37, No 3, pgs 630-643.

25. Platt C.M.R: 1973. Lidar and radiometric observations of cirrus clouds. *J.Atmos.Sci.* Vol 30. pgs 1191-1204.

26. Platt C.M.R: 1975. Infrared emissivity of cirrus- simultaneous satellite , Lidar and radiometric observations. *Quart.J.Roy.Meteor.Soc.* Vol 101, pgs 119-126.

27. Rawlins F and Foot J.S: 1990. Remotely sensed measurements of stratocumulus properties during FIRE using the C130 aircraft multi-channel radiometer. *J.Atmos.Sci.* Vol 47, No 21, pgs 2488-2503.
28. Ridgway W.L and Davies R: 1983. Interpretation of spectral reflectance from cloud tops. Conference on atmospheric radiation. American Meteorological Society. 1983, pgs 524-527.
29. Shifrin K.S: 1961. Milan, R.Inst.Geof., Geof.Pura Appl. Vol 48, pgs 129-137.
30. Smith W.L, Woolf H.M, Hayden C.M, Work D.Q and Mc Milan L.M: 1979. The Tiros-N operational vertical sounder, GARP topic No 58, pgs 1177-1187 *Bull.Am.Meteorol.Soc.*
31. Takano.Y and Liou.K.N: 1989. Solar radiative transfer in cirrus clouds. Part I. Single scattering and optical properties of hexagonal ice crystals. pg 224. Selected papers on scattering in the atmosphere. Edited by C. Bohren Optical Engineering Press. Vol 7 pgs 641.
32. Twomey.S and Seton K.J: 1980. Inferences of gross microphysical properties of clouds from spectral reflectance measurements. *J.Atmos.Sci.* Vol 37, pgs 1065-1069.
33. Van De Hulst H.C: 1957. Light scattering by small particles, John Wiley, New York.
34. Warren. S.G: 1984. Optical constants of ice from the ultraviolet to the microwave. *App.Opt.* Vol 23, No 8, pgs 1206-1225.
35. Winscombe W.J: 1980. Improved Mie scattering algorithms. *App.Opt.* Vol 19 pgs 1505-1509.

36. Webster P.J and Stephens G.L: 1984. Cloud-Radiation interaction and the climate problem. Cambridge: Global Climatology:1984:63-68.

37. Yamamoto G. Masayuki T and Shoji A: (1970). Radiative transfer in water clouds in the infrared region. Jour.Atmos.Sci. Vol 27. pgs 282-292.

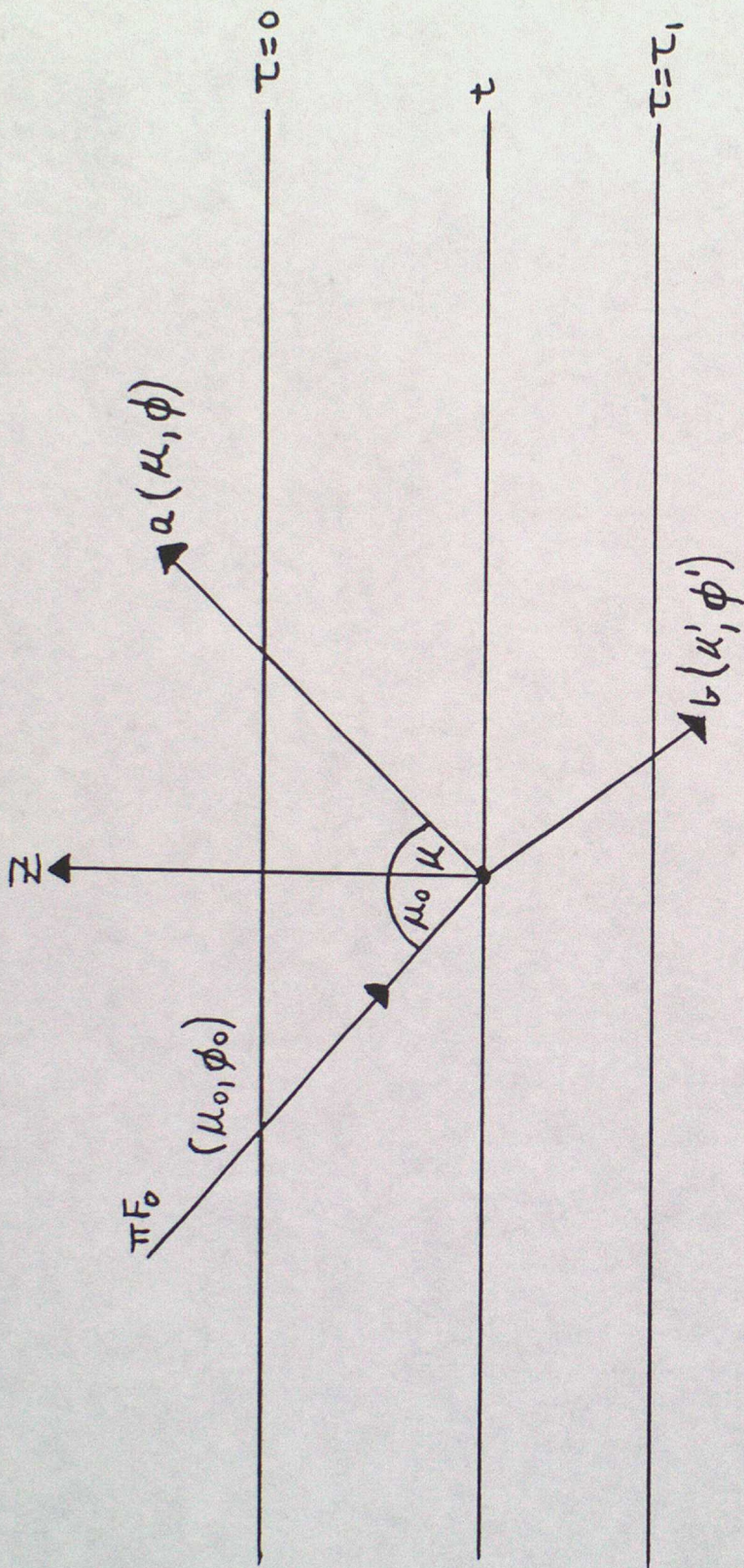


Figure 1. Illustration of scattering for an incident flux πF_0 of radiation on a plane-parallel atmosphere. Single scattering is shown as a and multiple scattering as b.

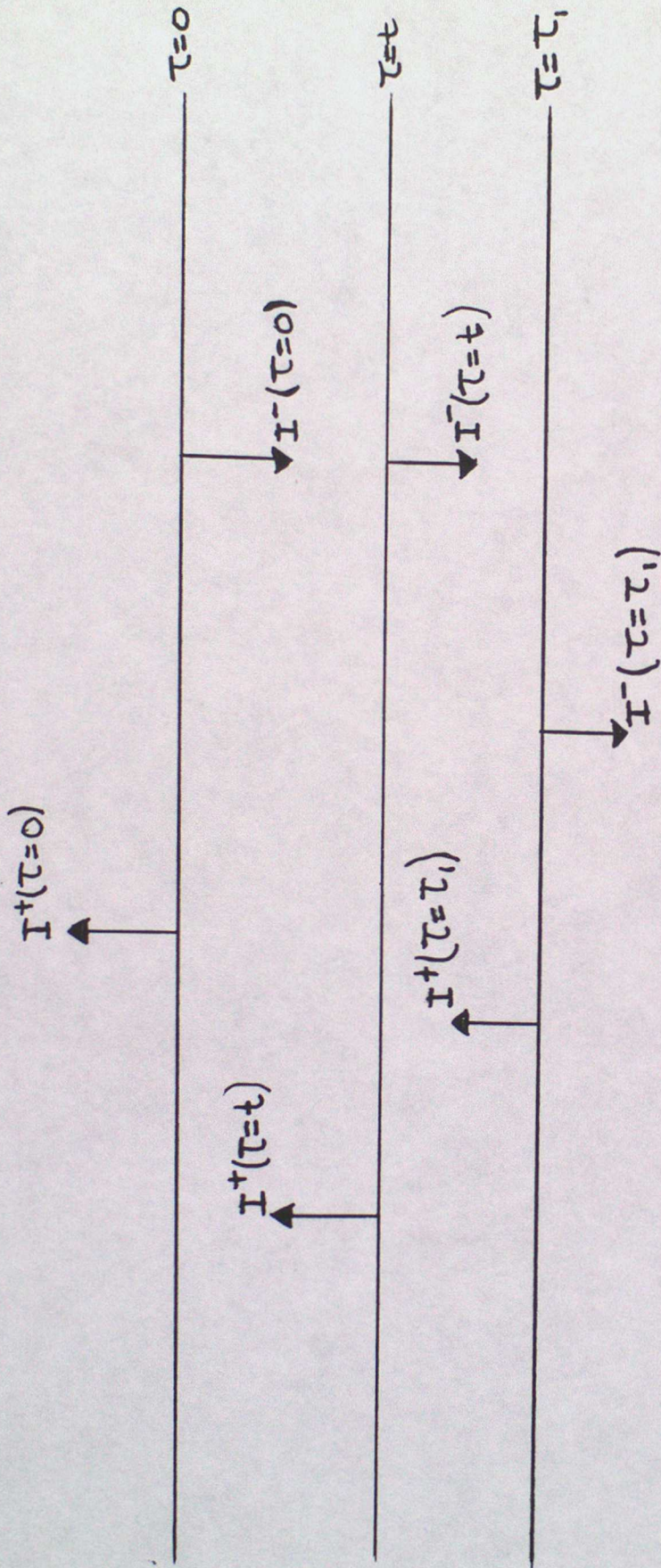


Figure 2. Illustration of the upward and downward intensities (neglecting angular dependence) in a plane-parallel atmosphere.

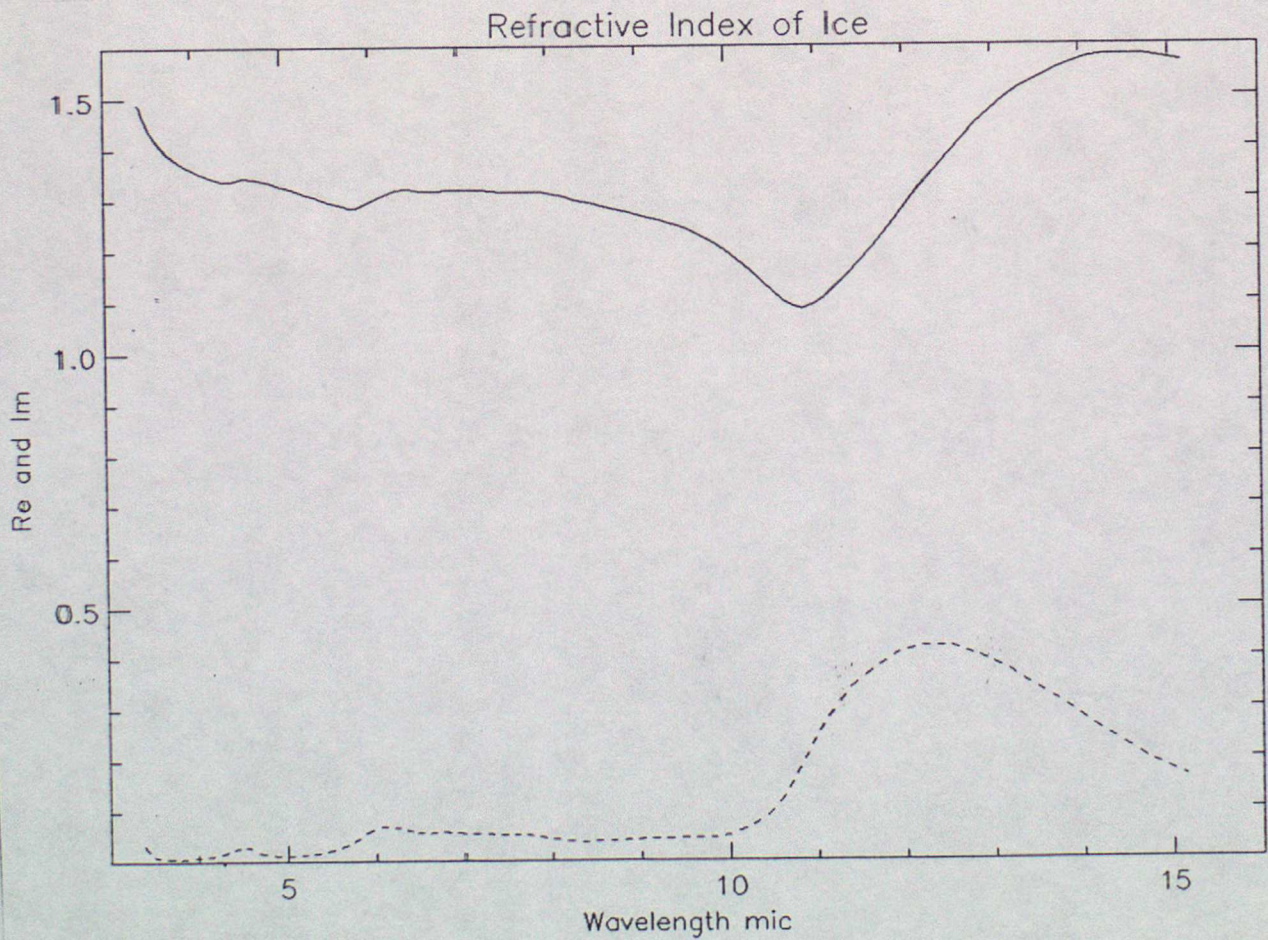
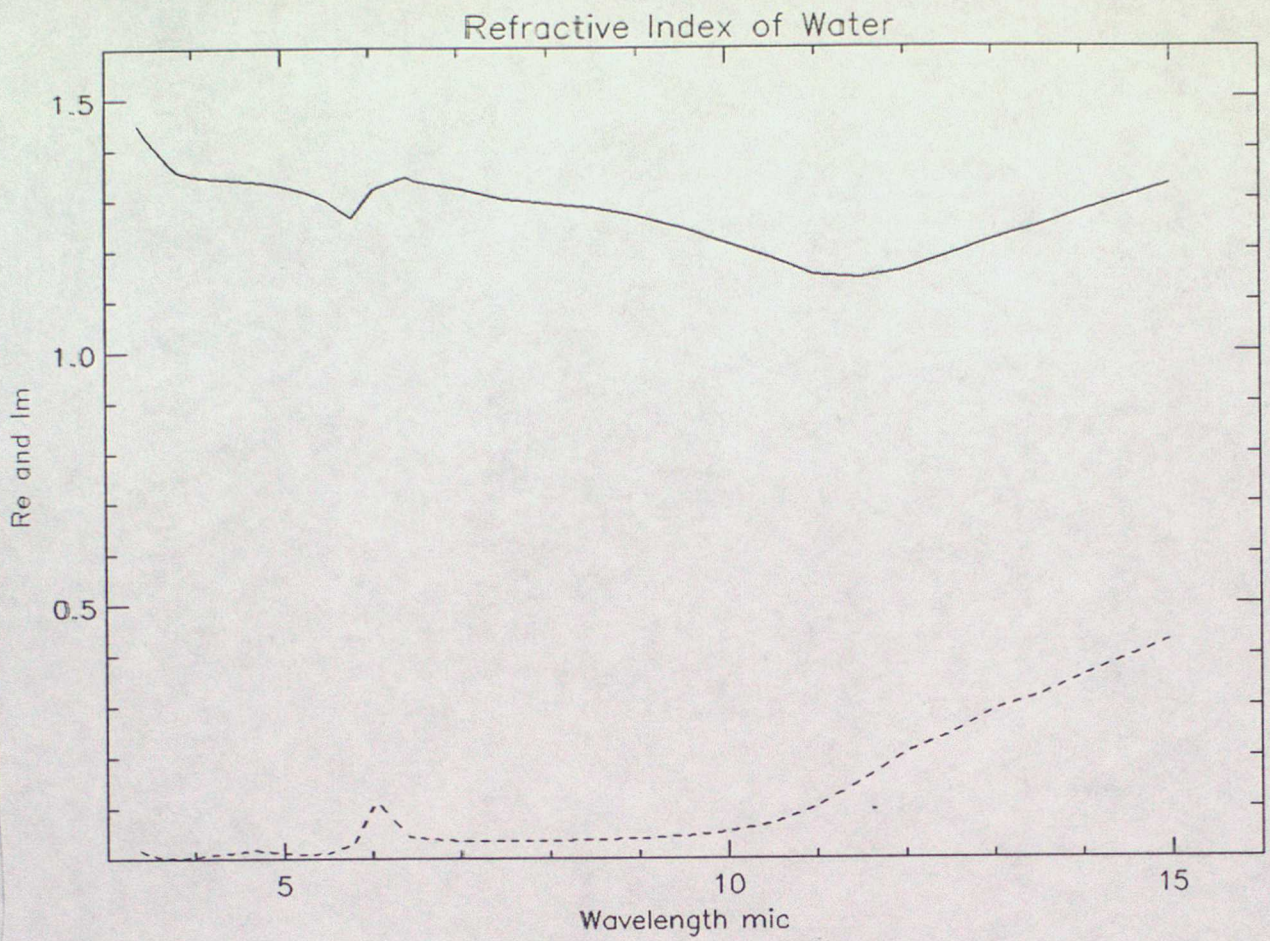


Figure 3. The real and imaginary parts of the refractive index of water and ice. From Irvine and Pollack (1968) and Warren (1984) respectively.

Figure 4. The scattering and absorption coefficients for a single water droplet.

Radius of Droplet = 3.5 microns

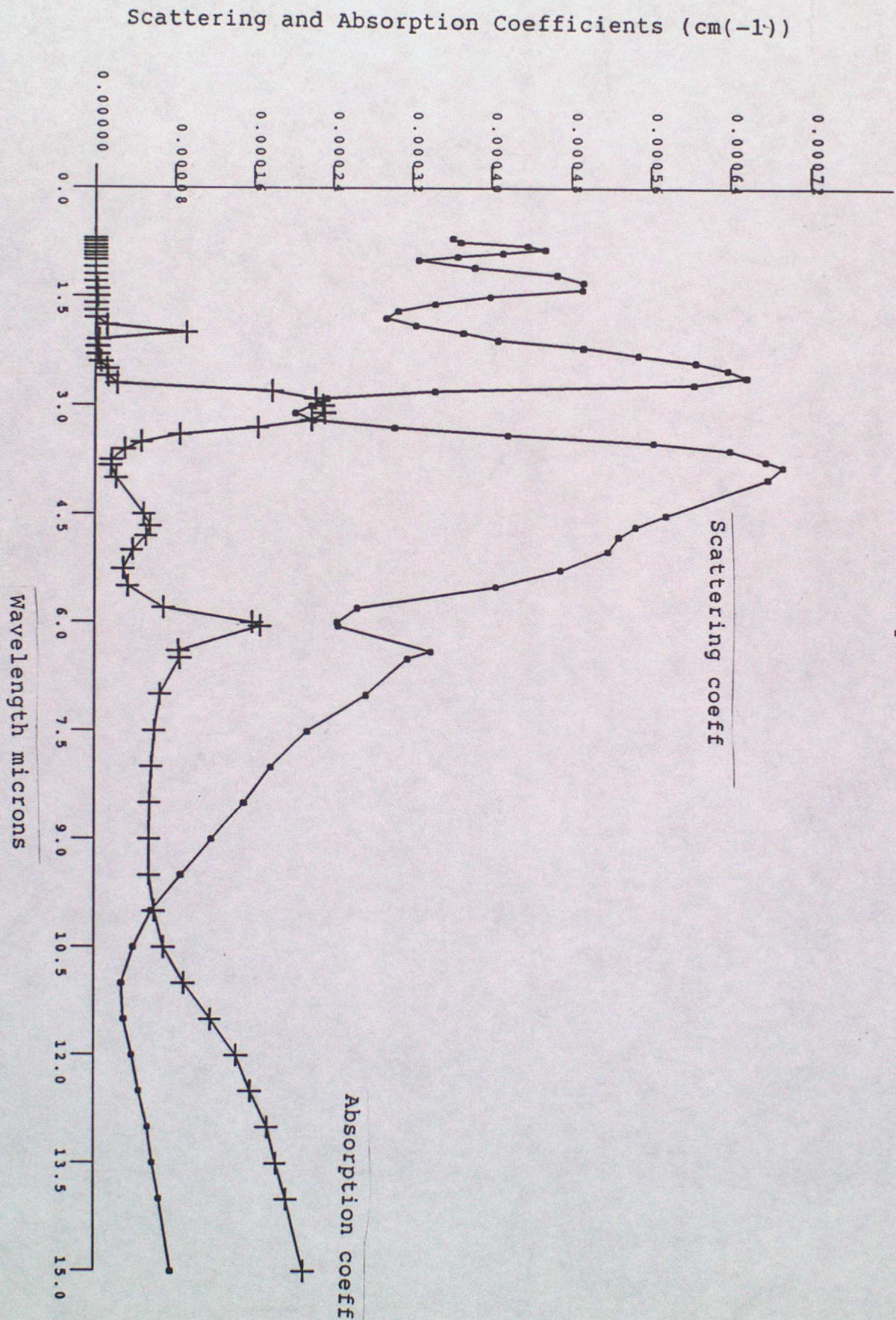
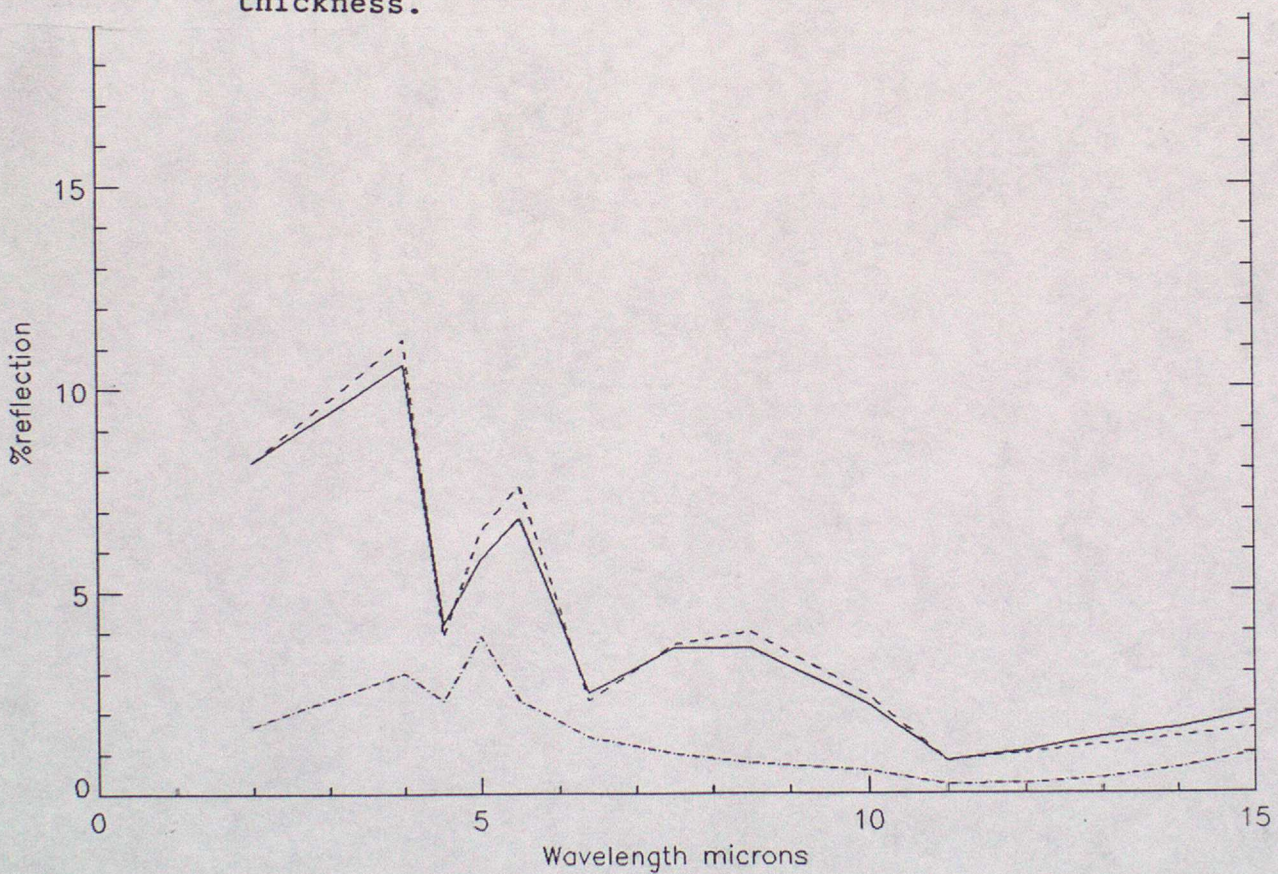


Figure 5. Comparison of reflectance as calculated by Foot and Author for a typical water cloud of semi- infinite and infinite thickness.



$R_{mod} = 9$ microns $N = 100 \text{ cm}^{-3}$. Droplets described by the Modified Gamma Function after Deirmendjian (1969).

Broken Line: Author (two-stream approx)

Full Line: Foot (after Chandreskhar)

Dotted and Broken Line: Author (Single Particle Scattering)

Figure 6. Comparison of single scattering albedo, extinction and scattering efficiencies for a water droplet of modal radius 9 microns.

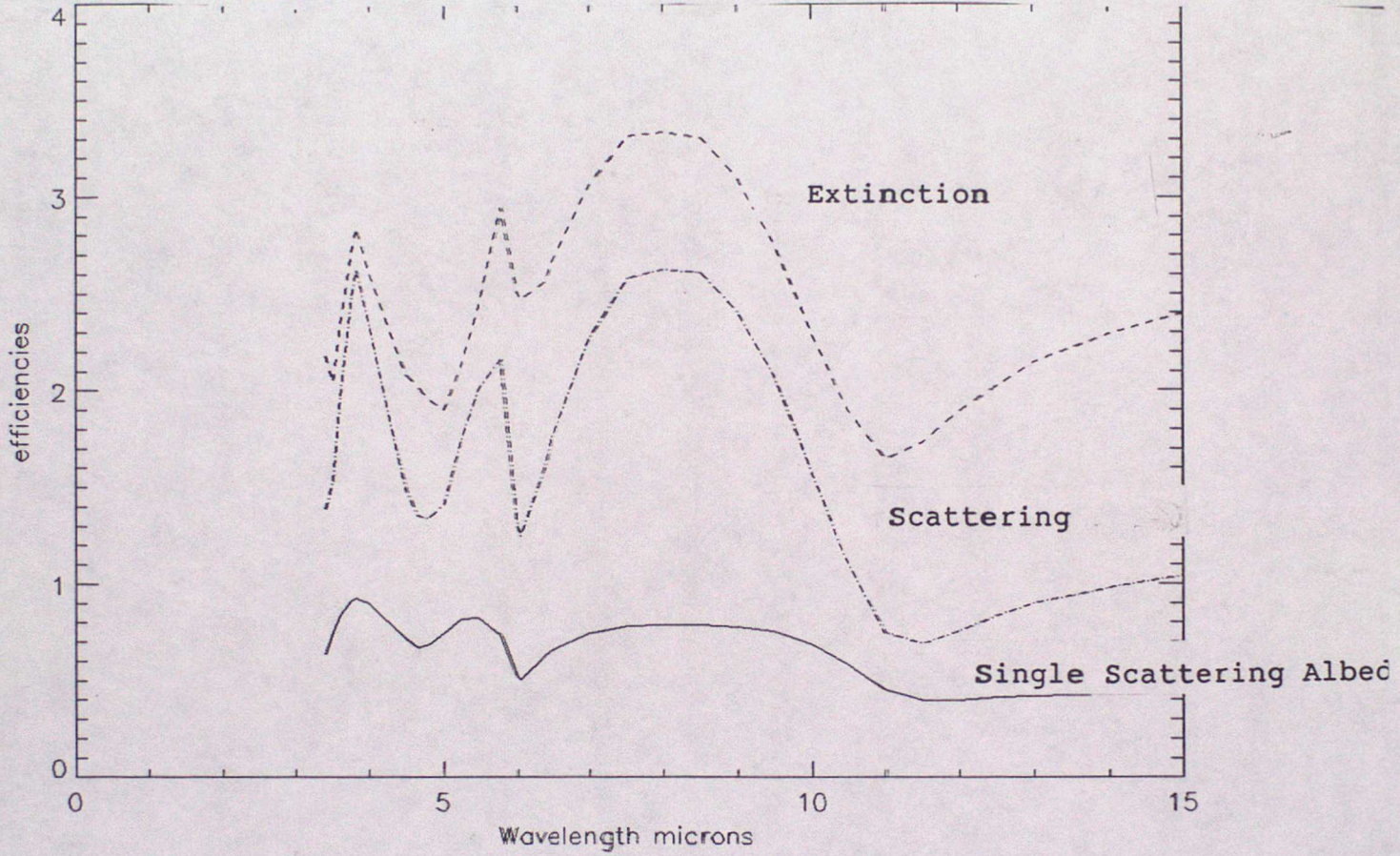
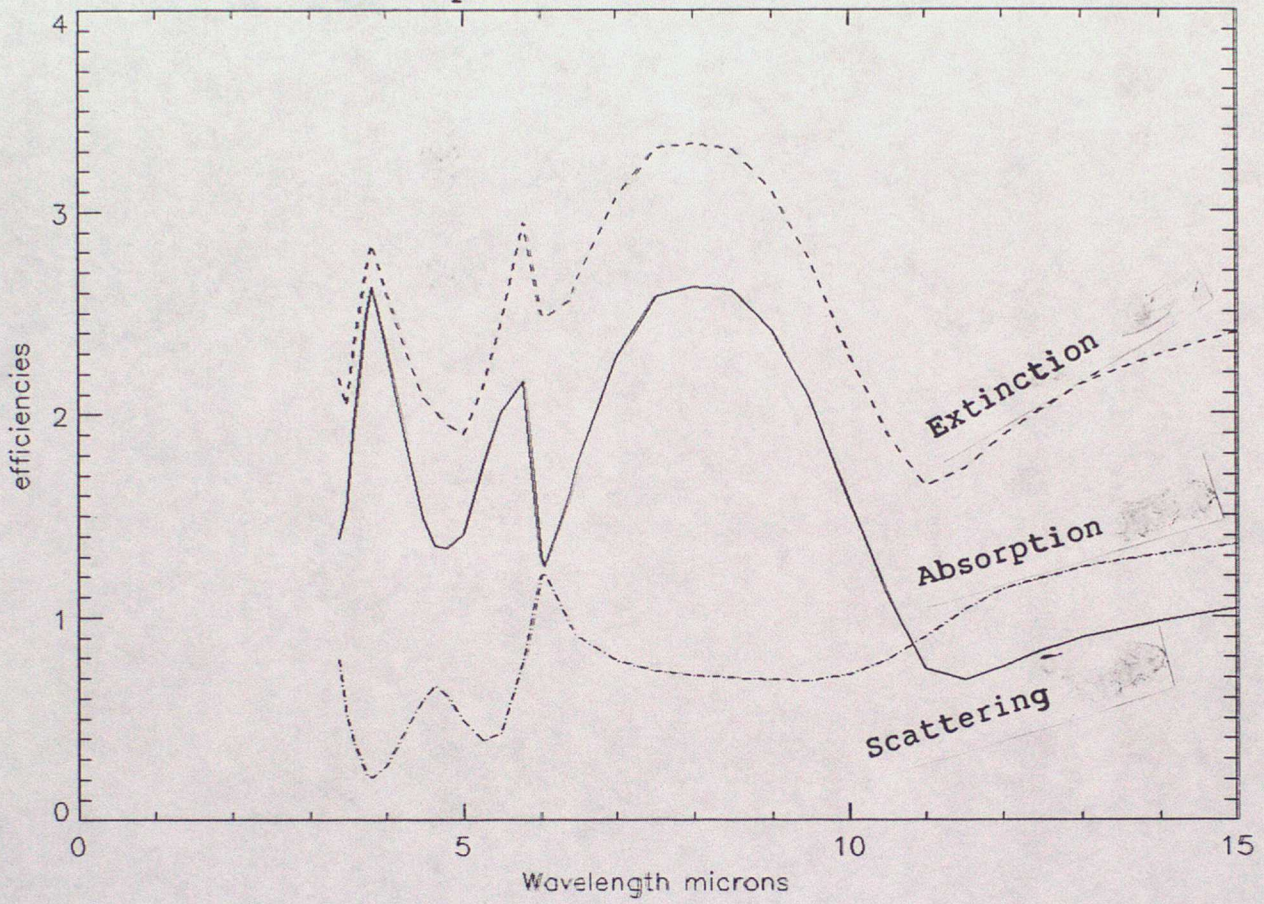


Figure 7. Comparison of absorption, extinction and scattering efficiencies for a water droplet of modal radius 9 microns.



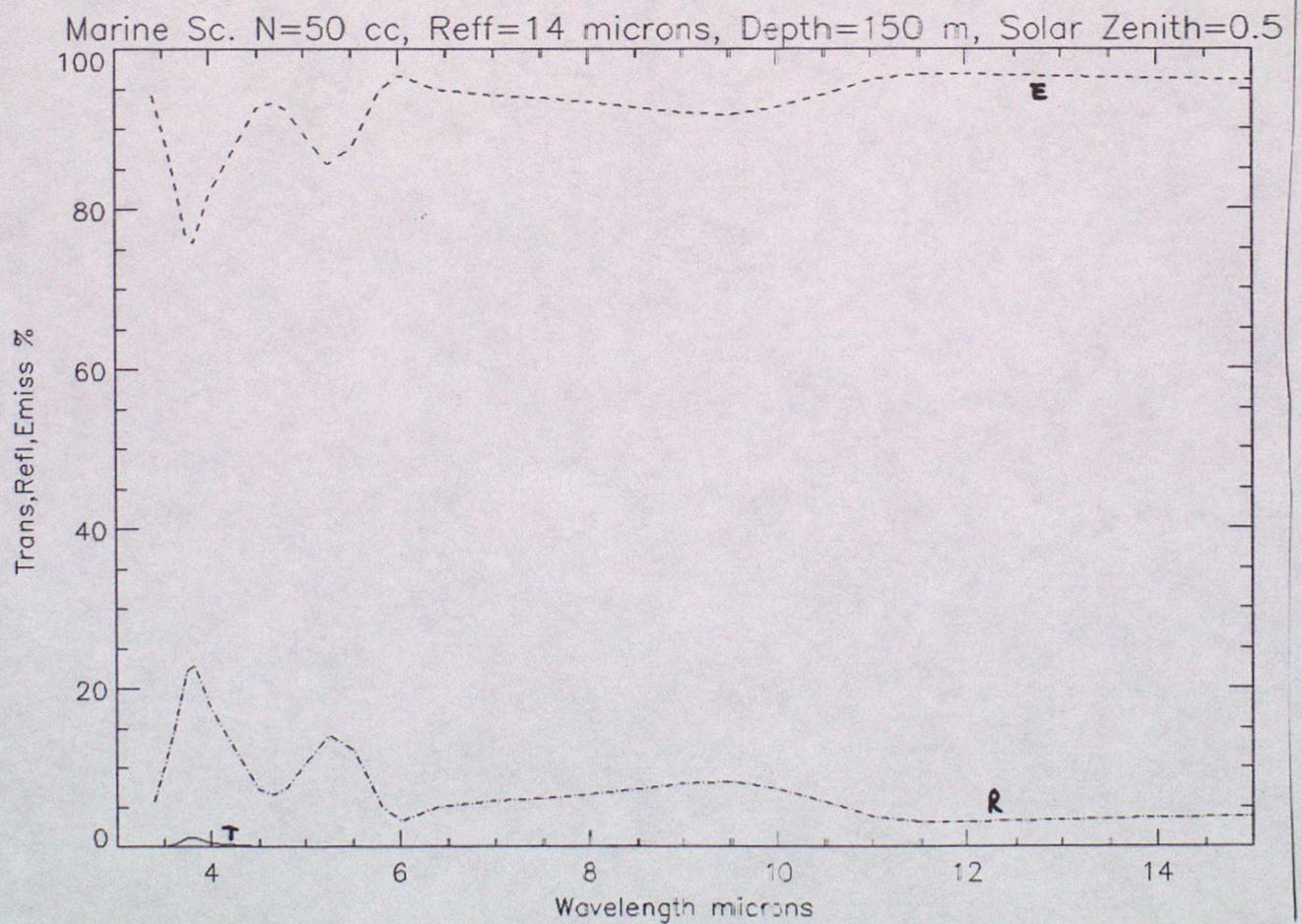
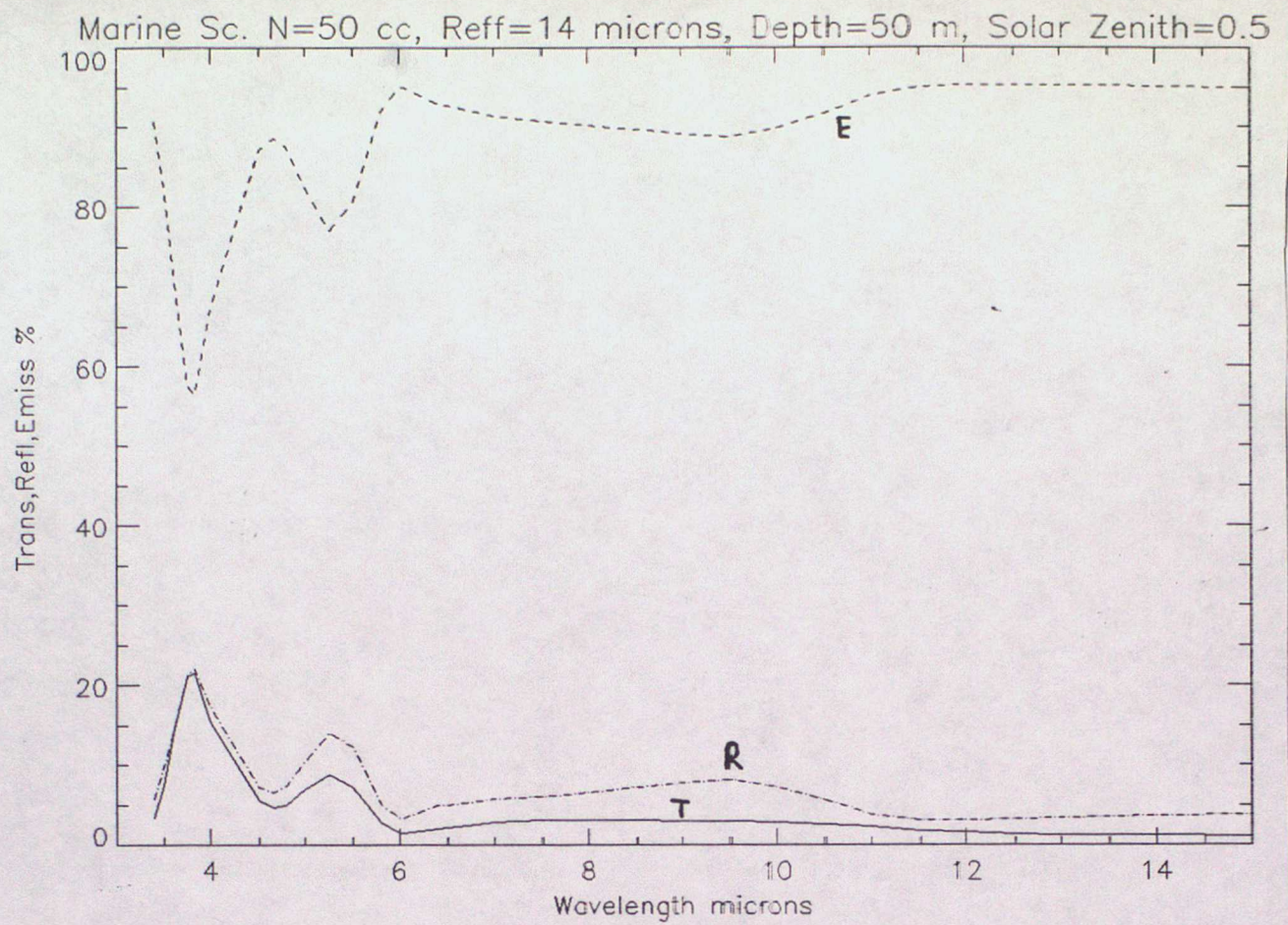


Figure 8. Radiative properties of marine stratocumulus

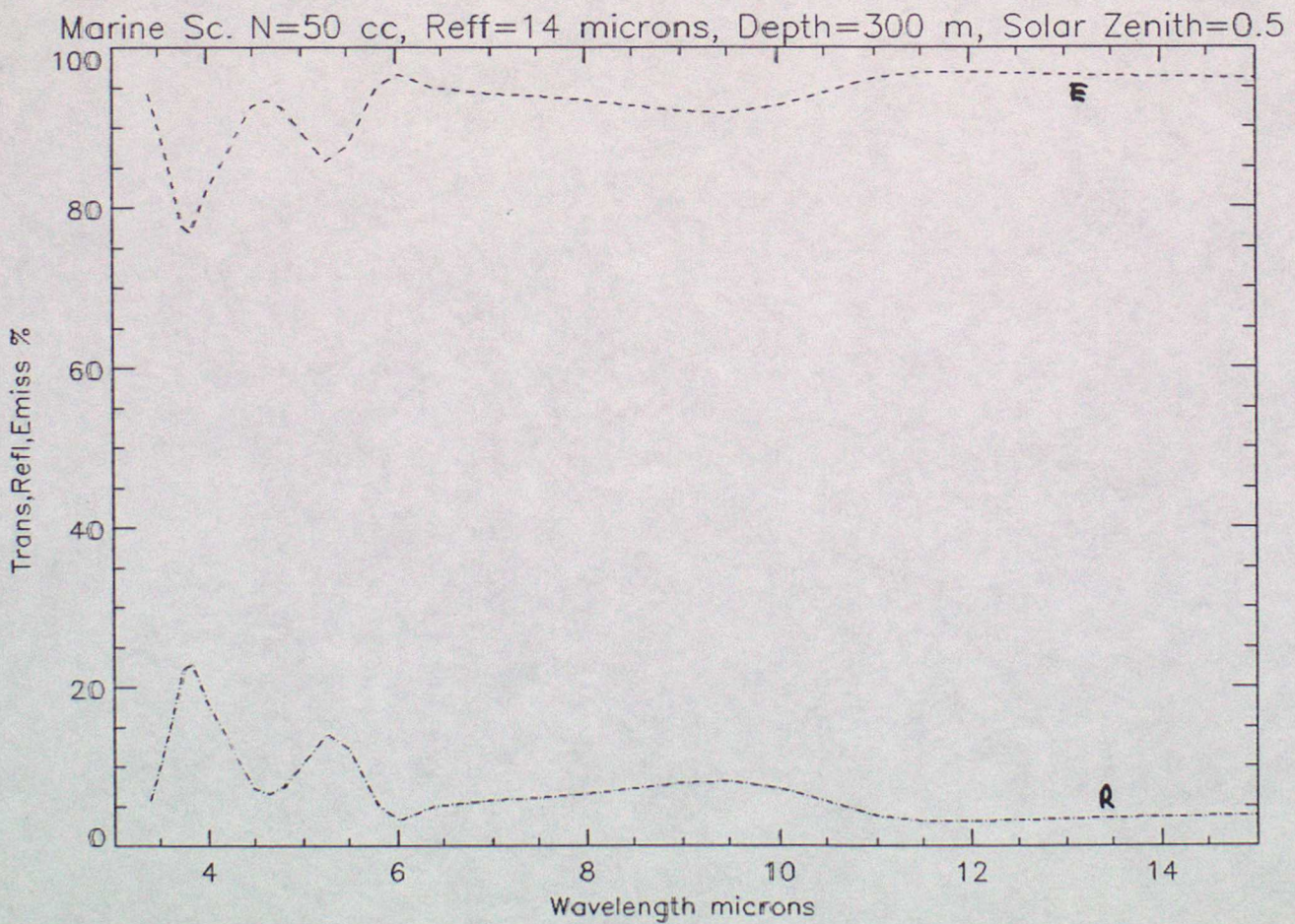
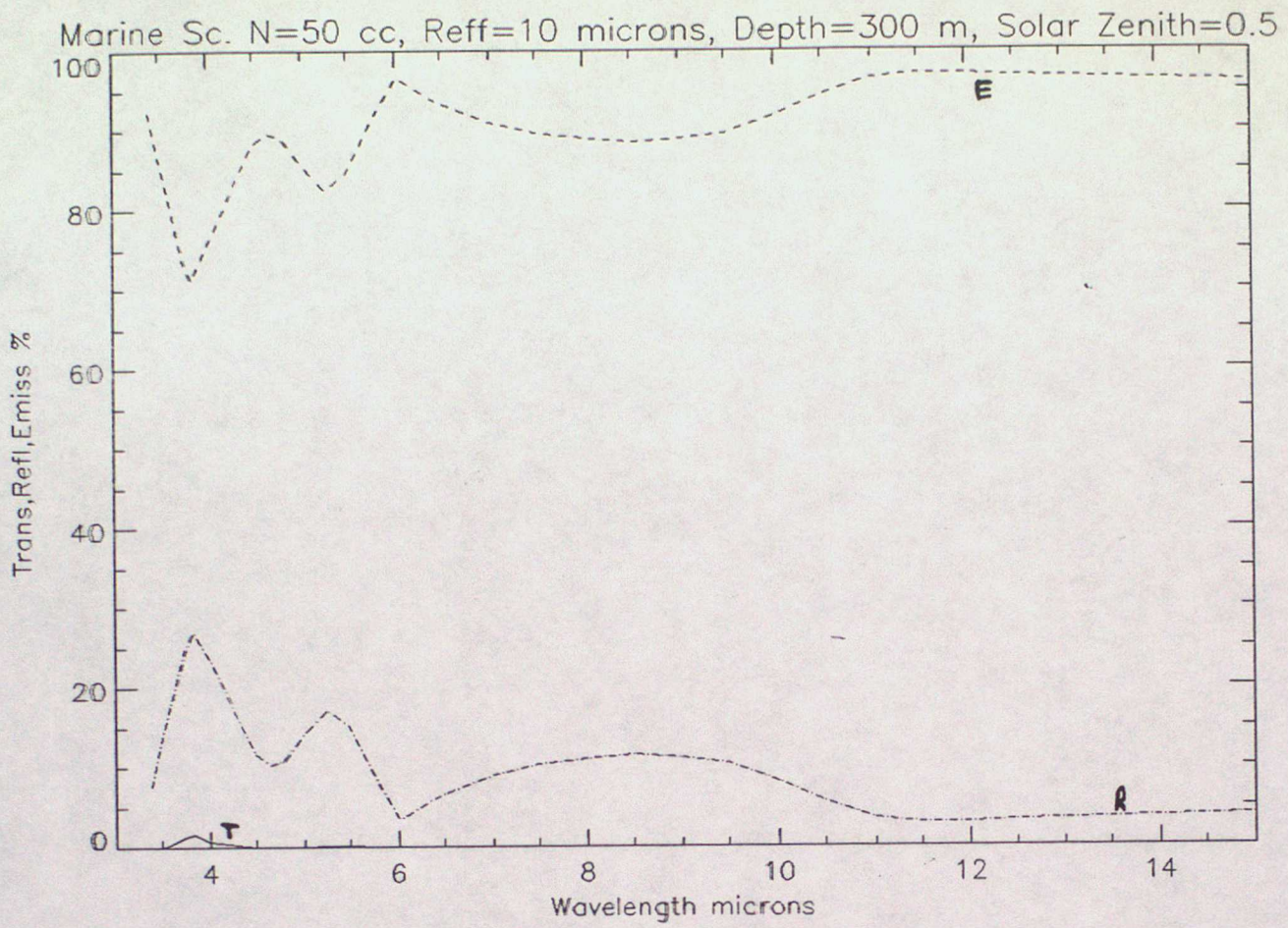


Figure 9. Radiative properties of marine stratocumulus

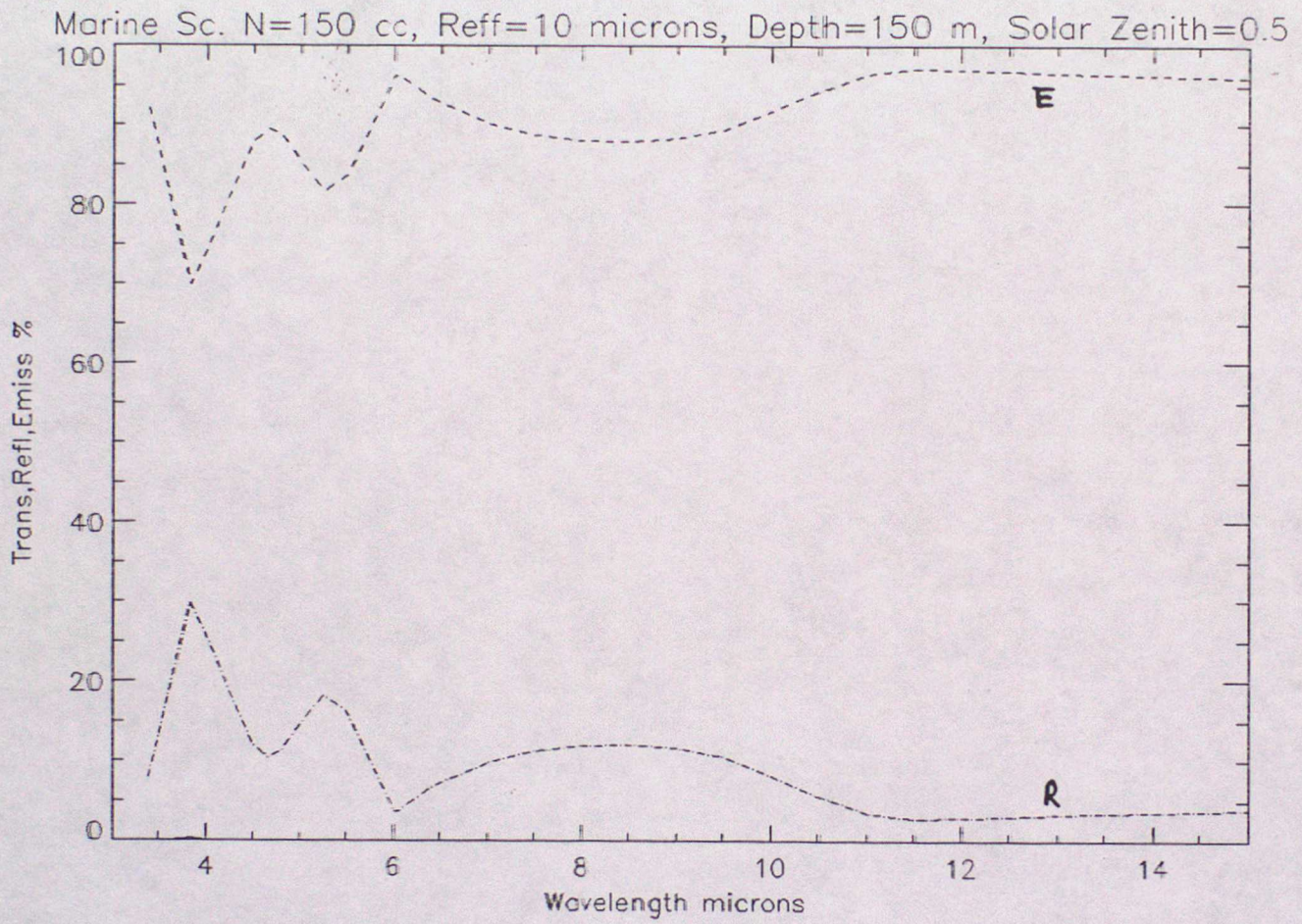


Figure 10. Radiative properties of marine stratocumulus

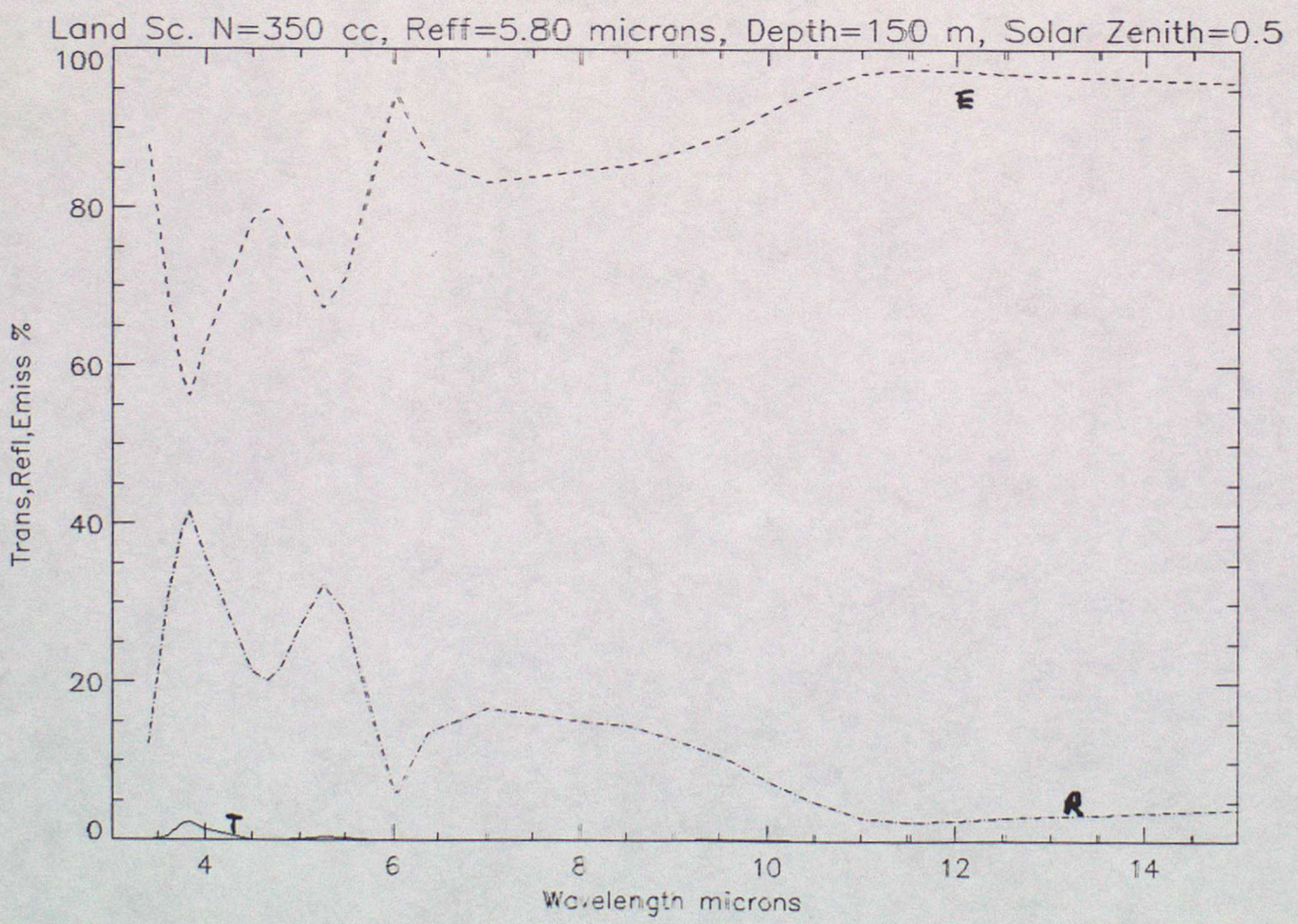
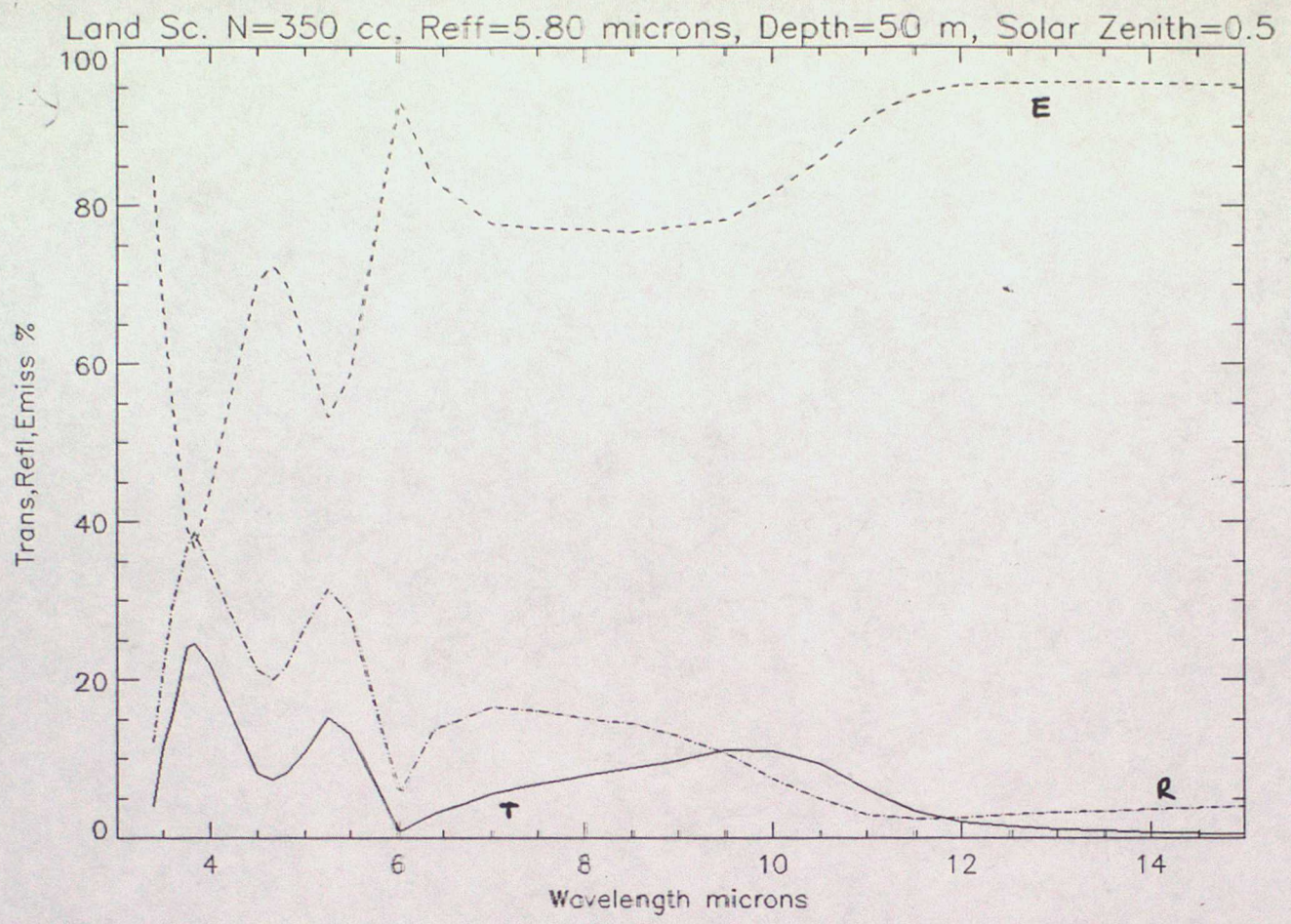


Figure 11. Radiative properties of land stratocumulus

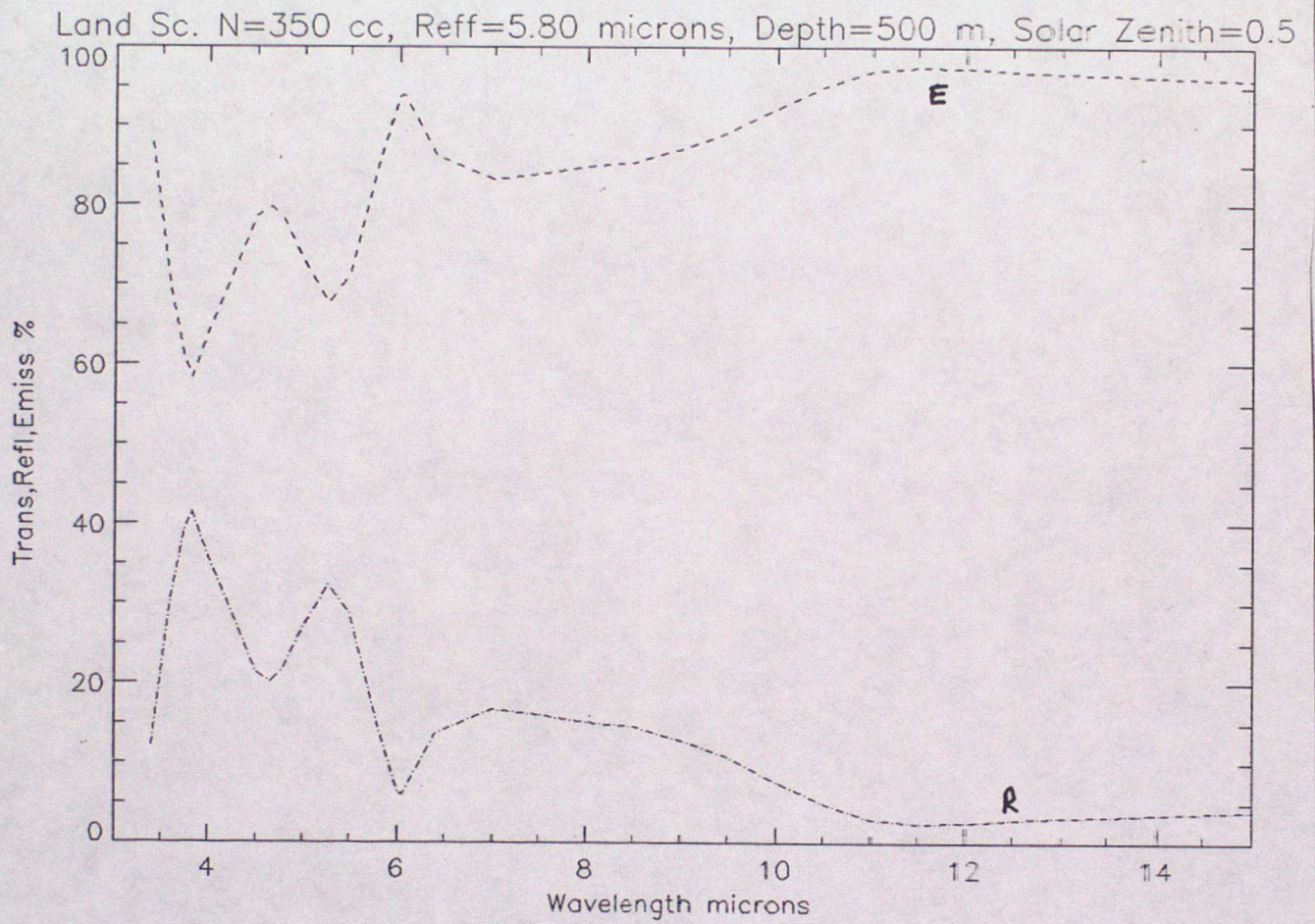


Figure 12. Radiative properties of land stratocumulus

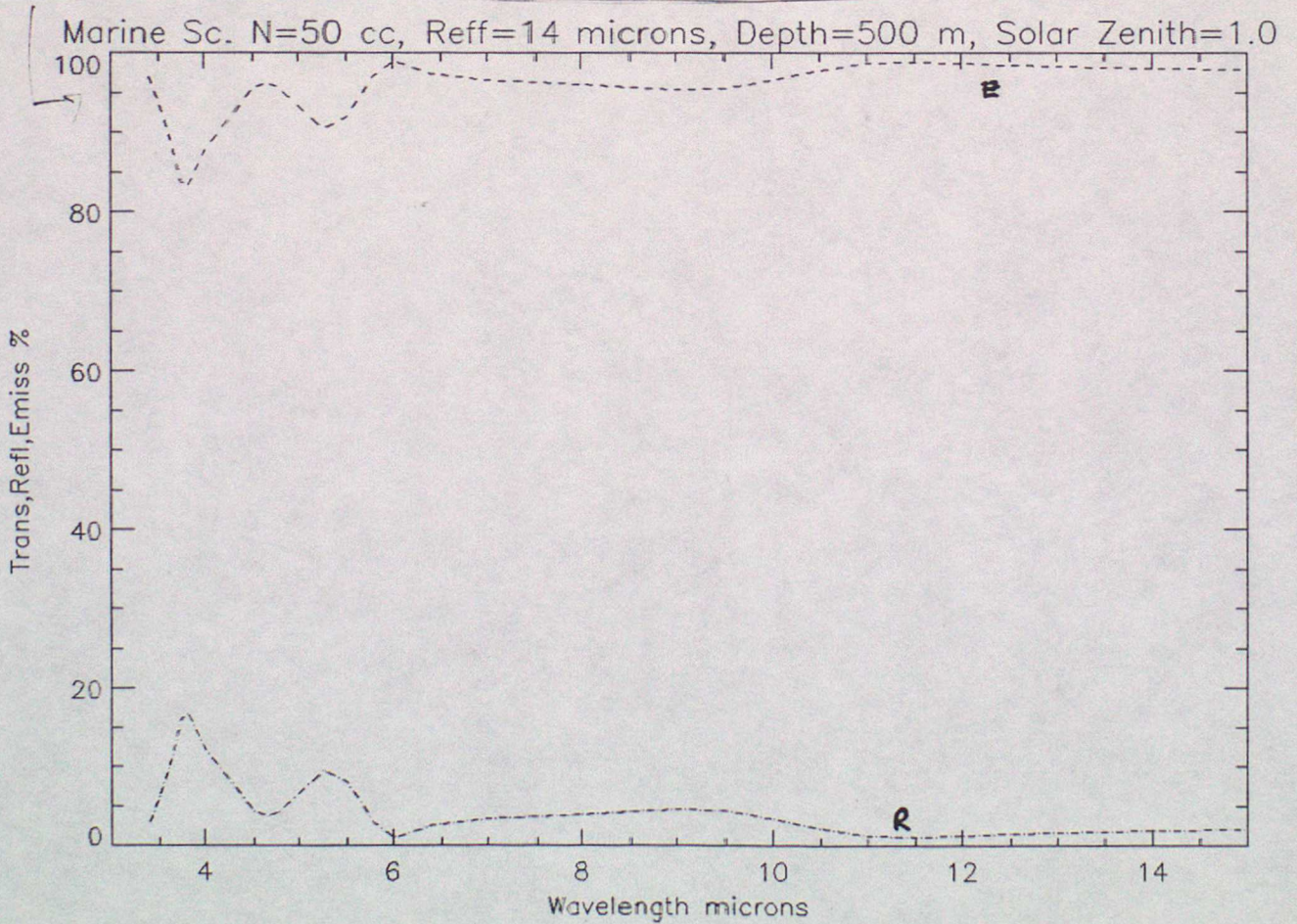
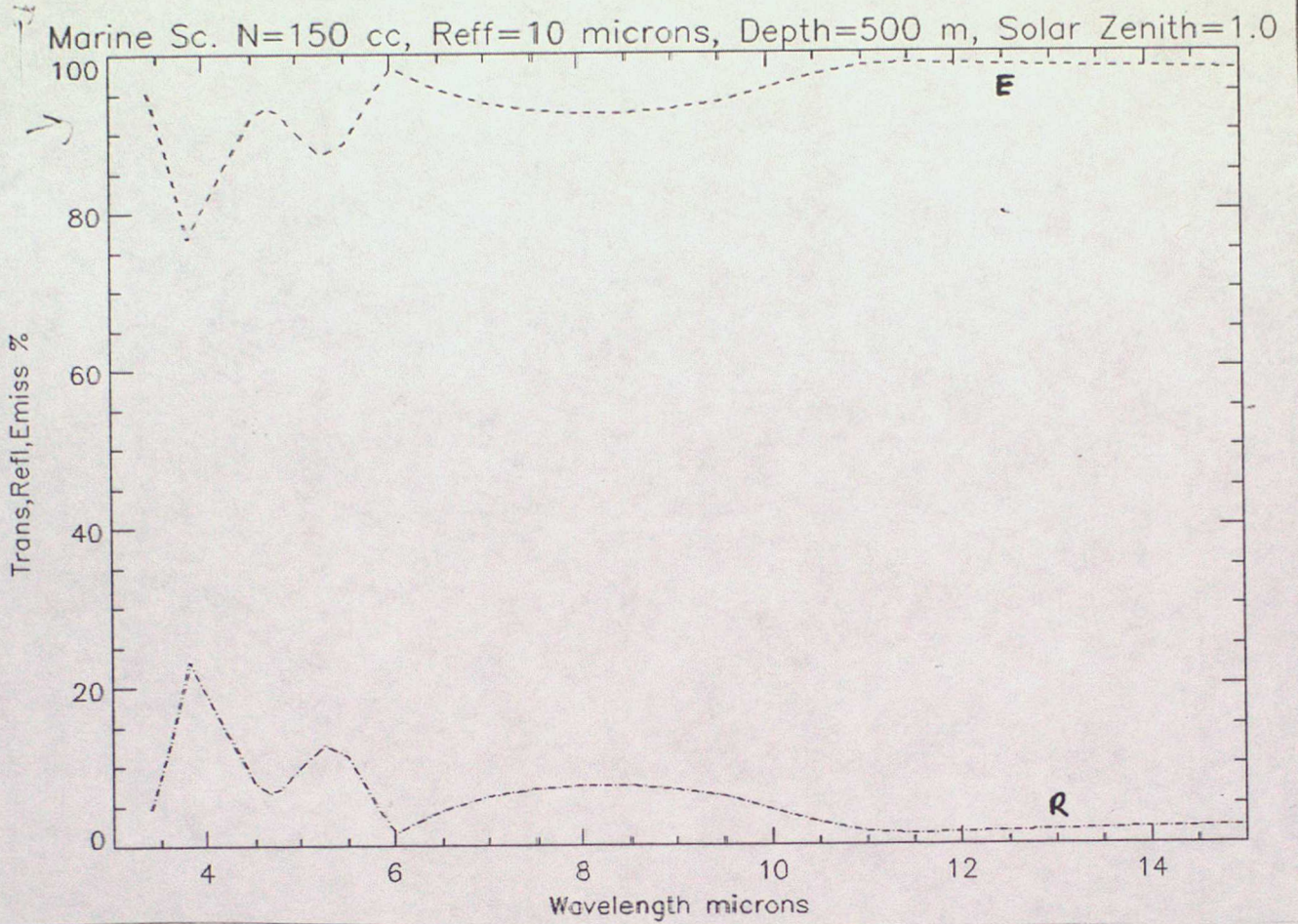


Figure 13. Radiative properties of marine stratocumulus

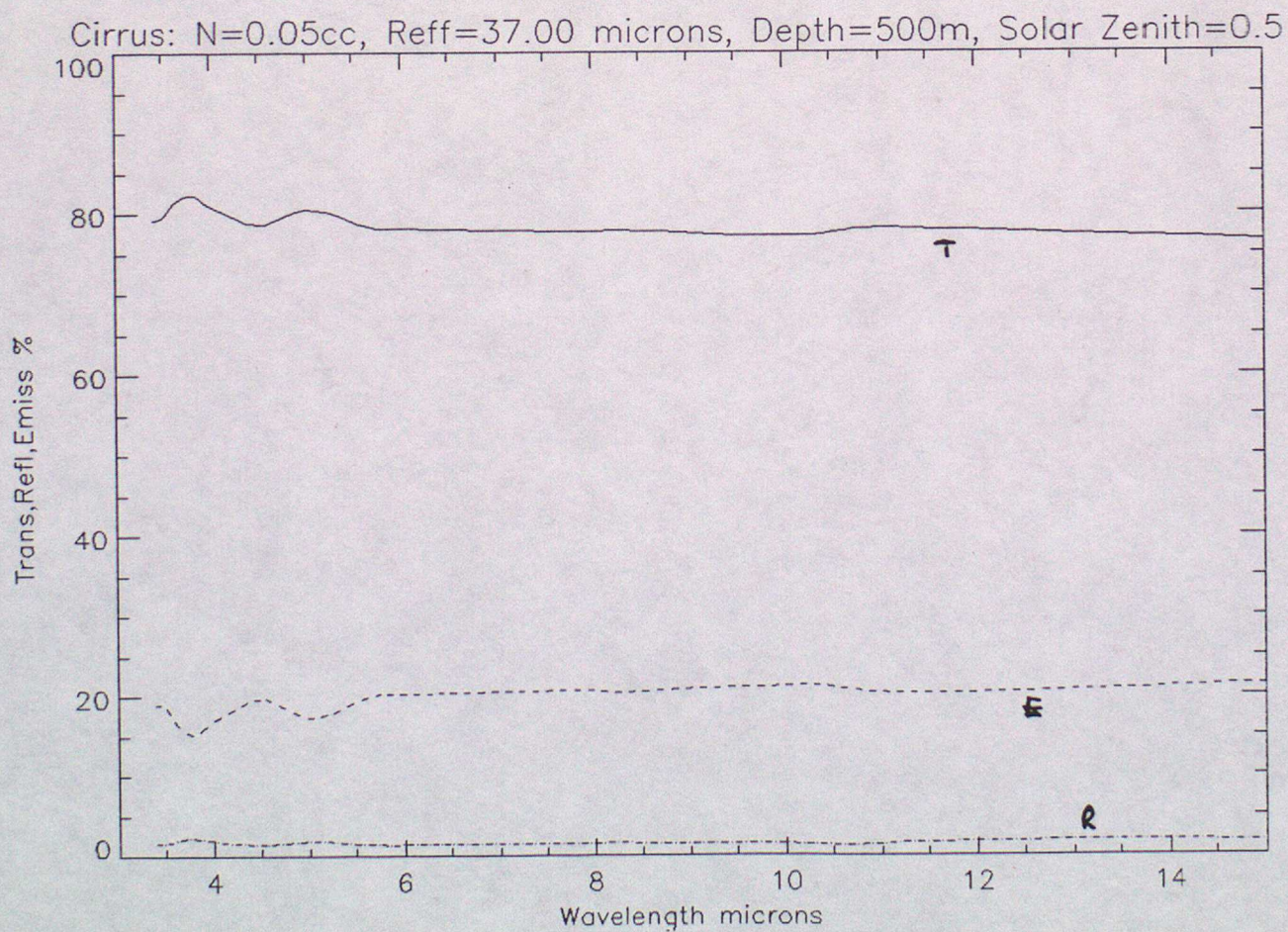
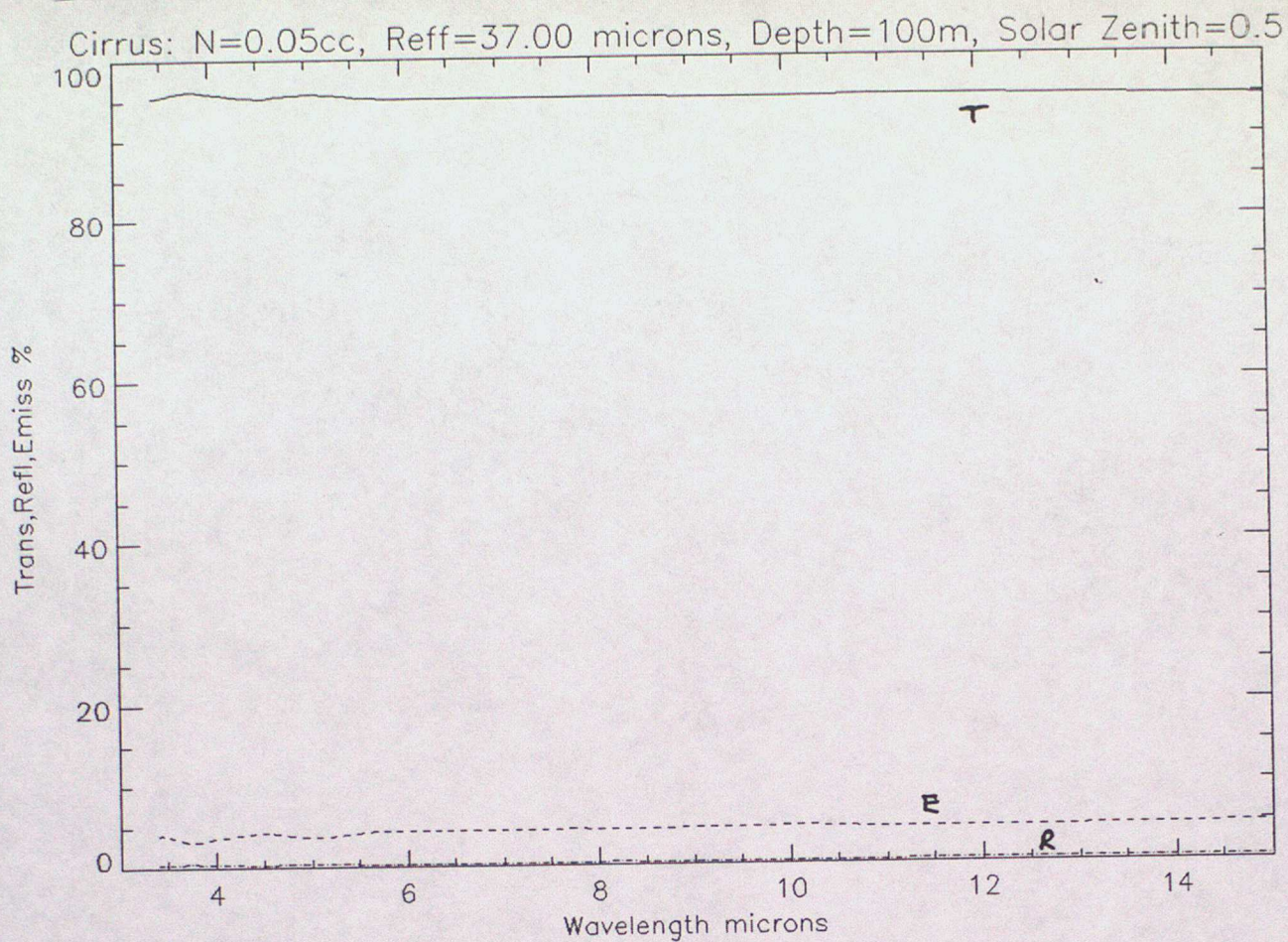
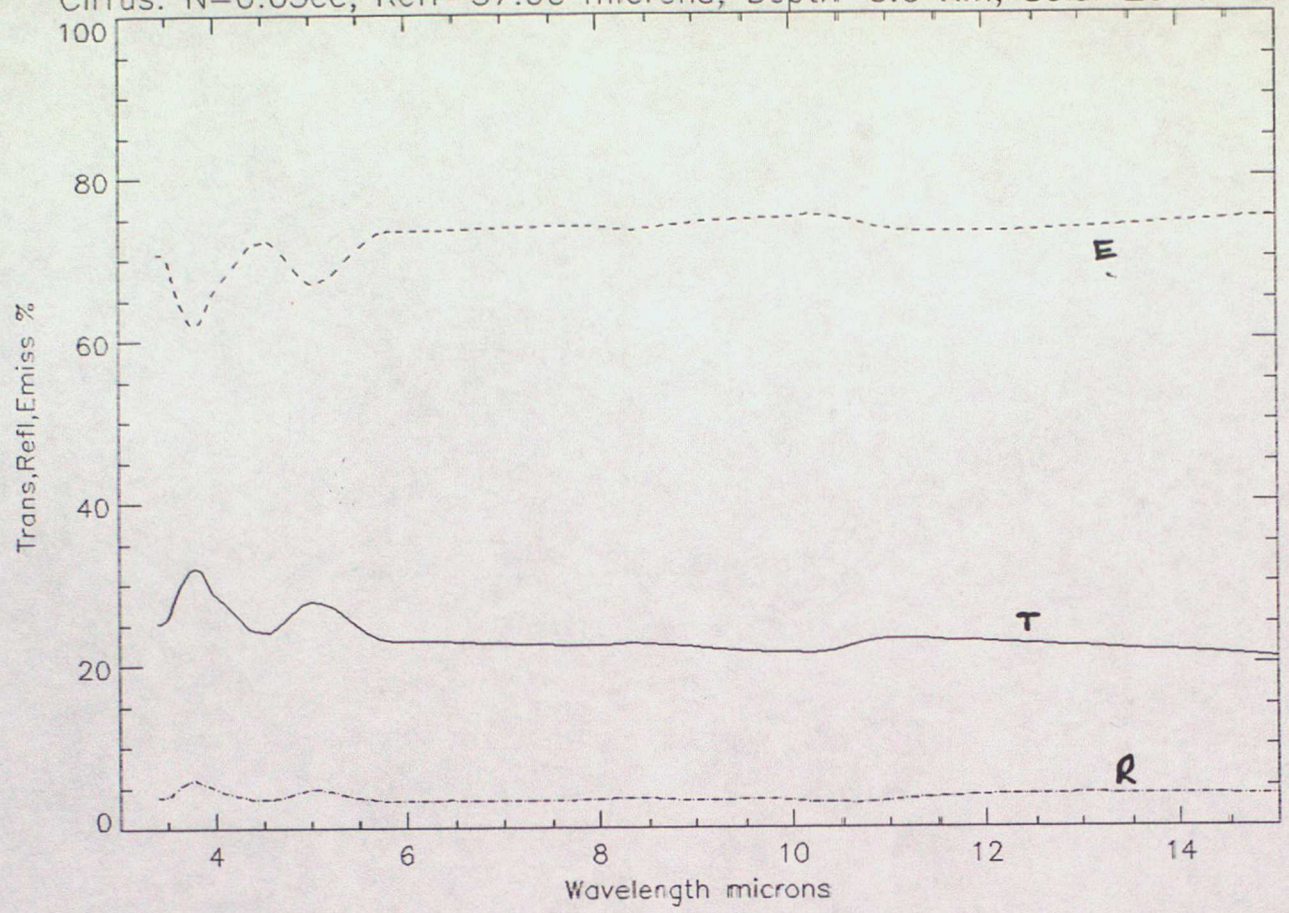


Figure 14. Radiative properties of cirrus

Cirrus: $N=0.05\text{cc}$, $\text{Reff}=37.00$ microns, $\text{Depth}=3.0$ Km, $\text{Solar Zenith}=0.5$



Cirrus: $N=0.1\text{cc}$, $\text{Reff}=19.00$ microns, $\text{Depth}=500\text{m}$, $\text{Solar Zenith}=0.5$

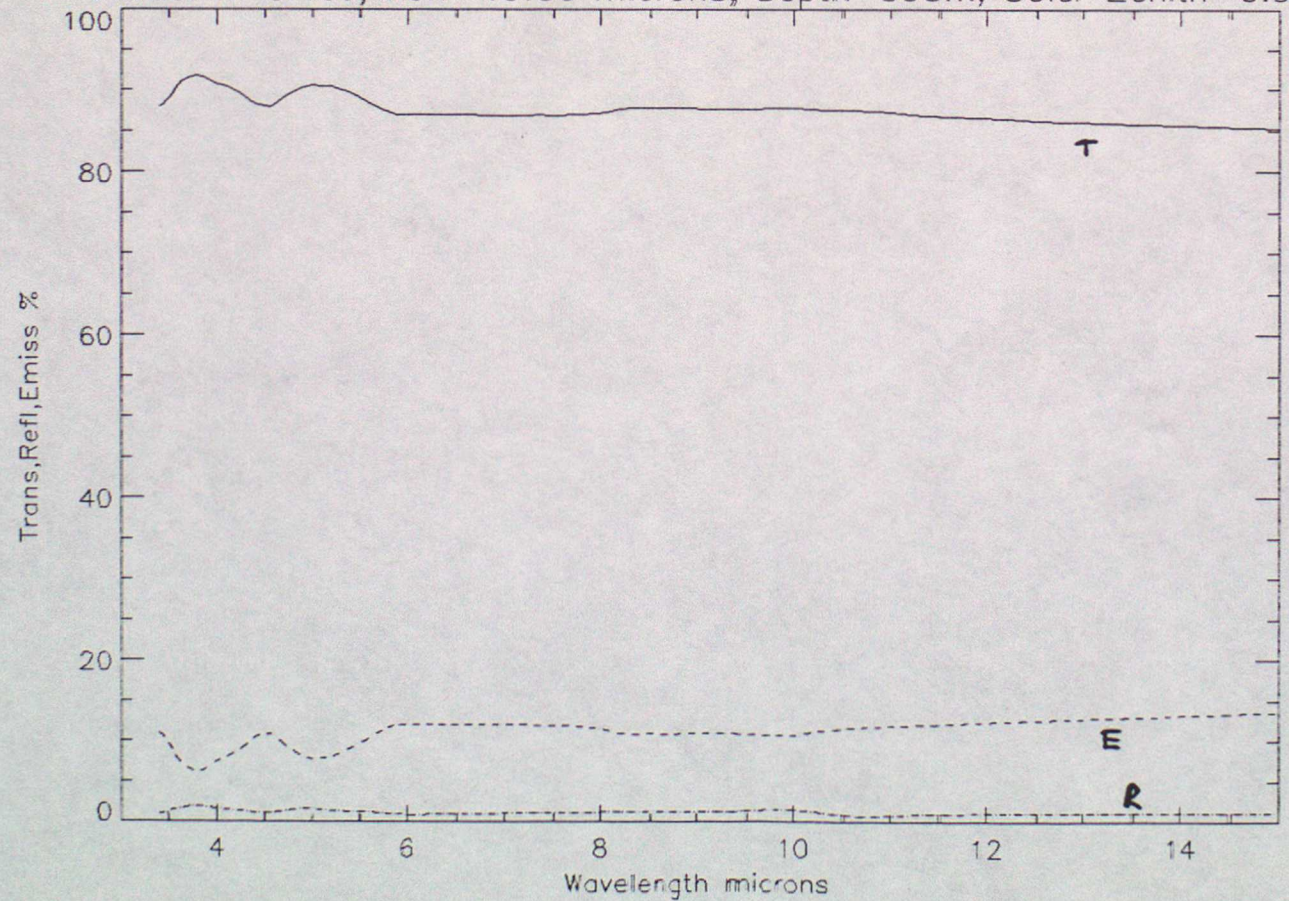


Figure 15. Radiative properties of cirrus

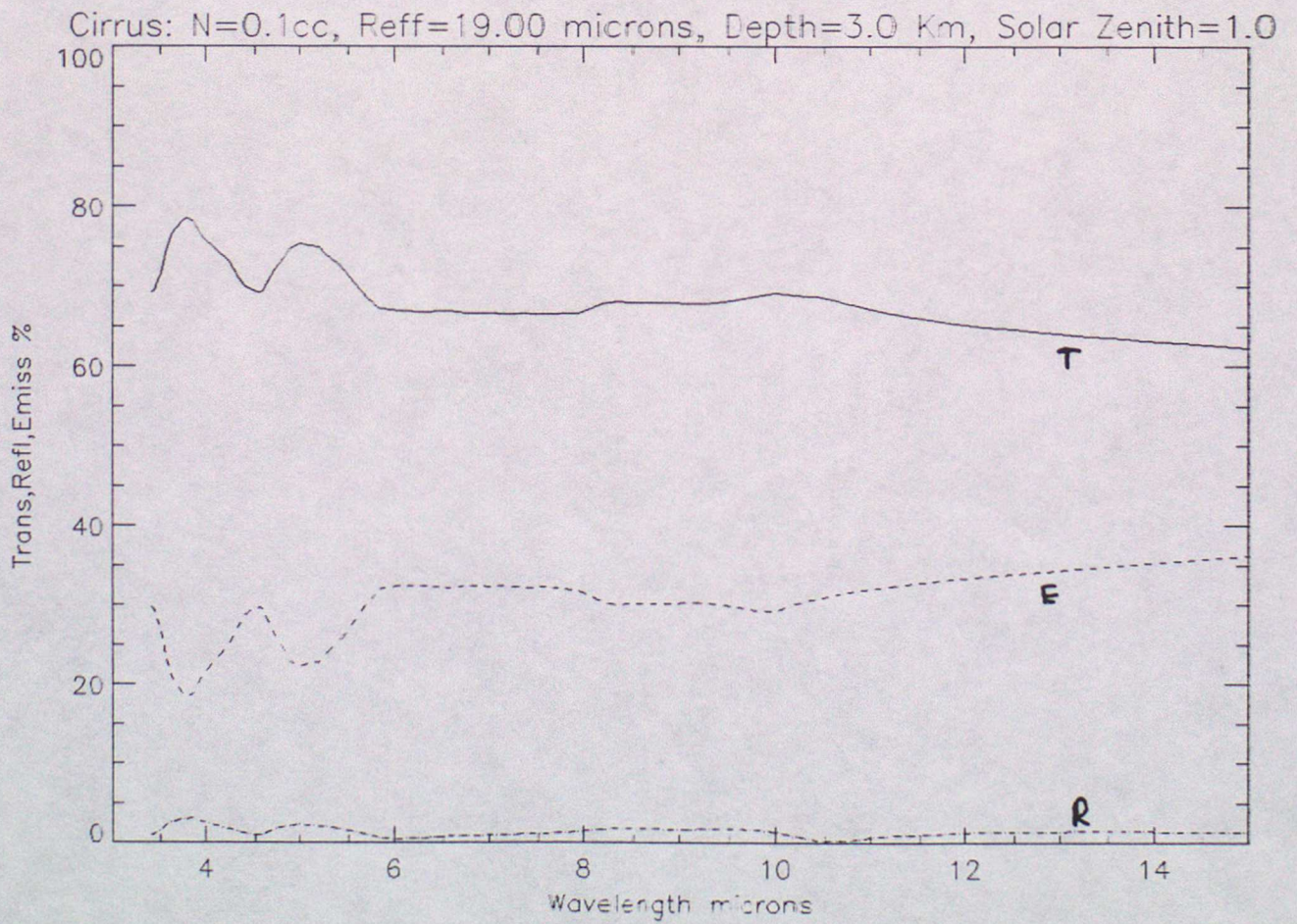
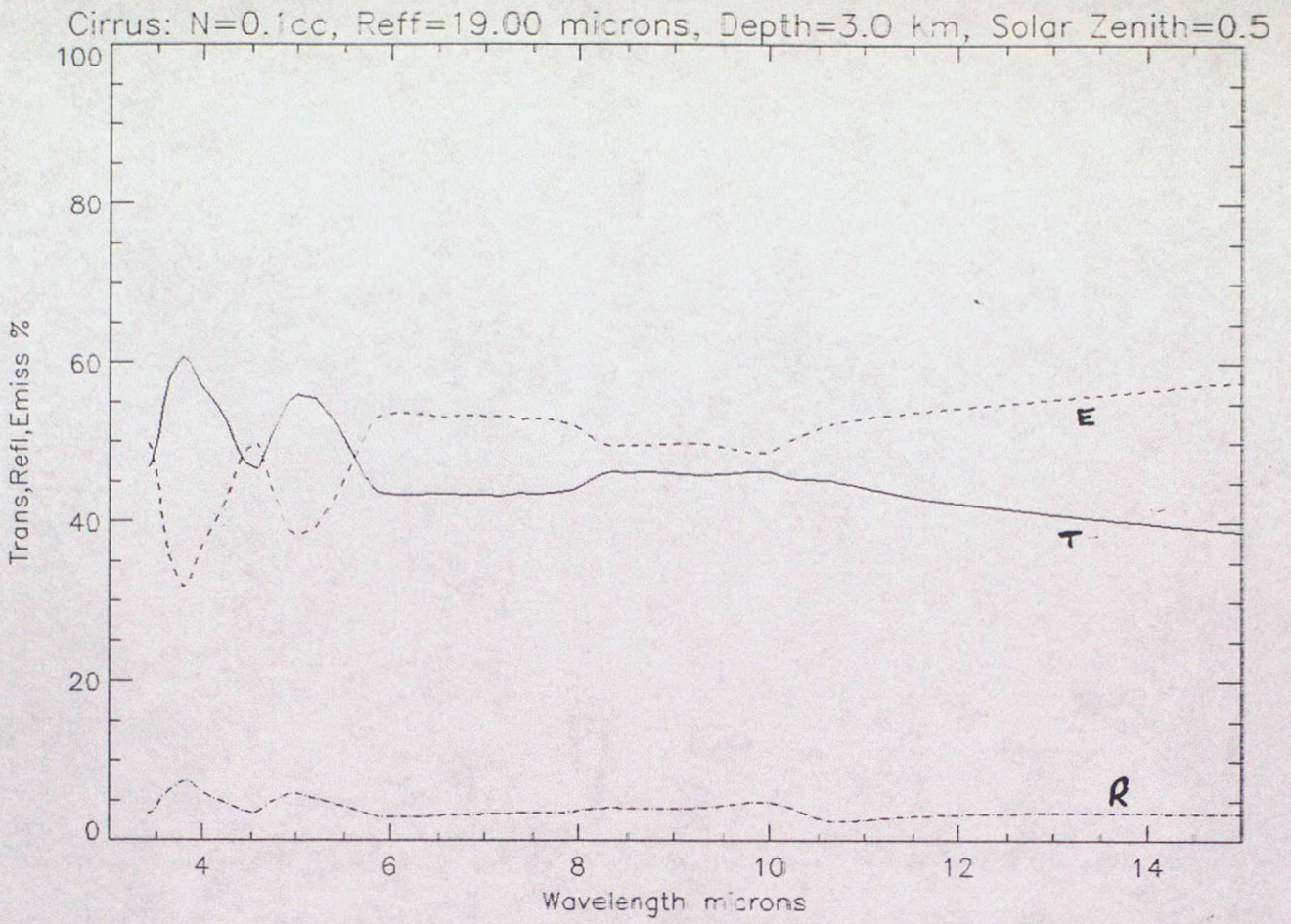


Figure 16. Radiative properties of cirrus

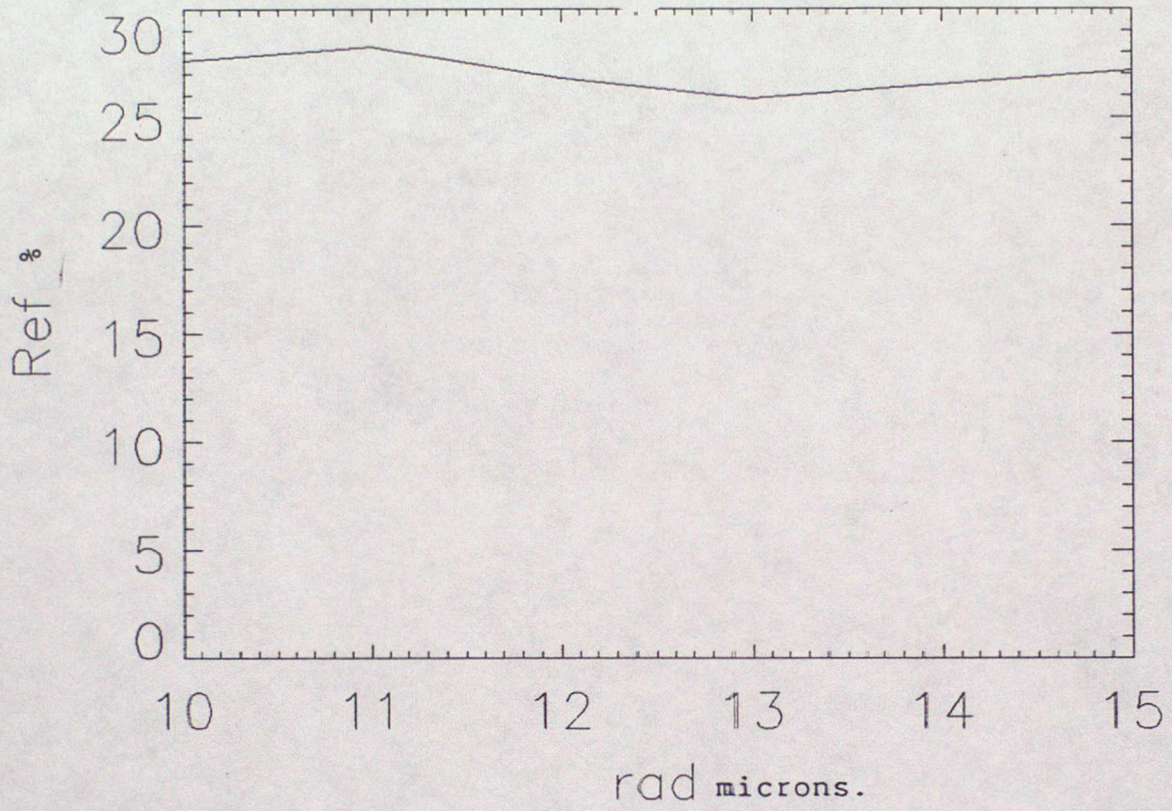


Figure 17. sensitivity of reflectance on radius of Droplet at 0.7 microns for a fixed optical depth.

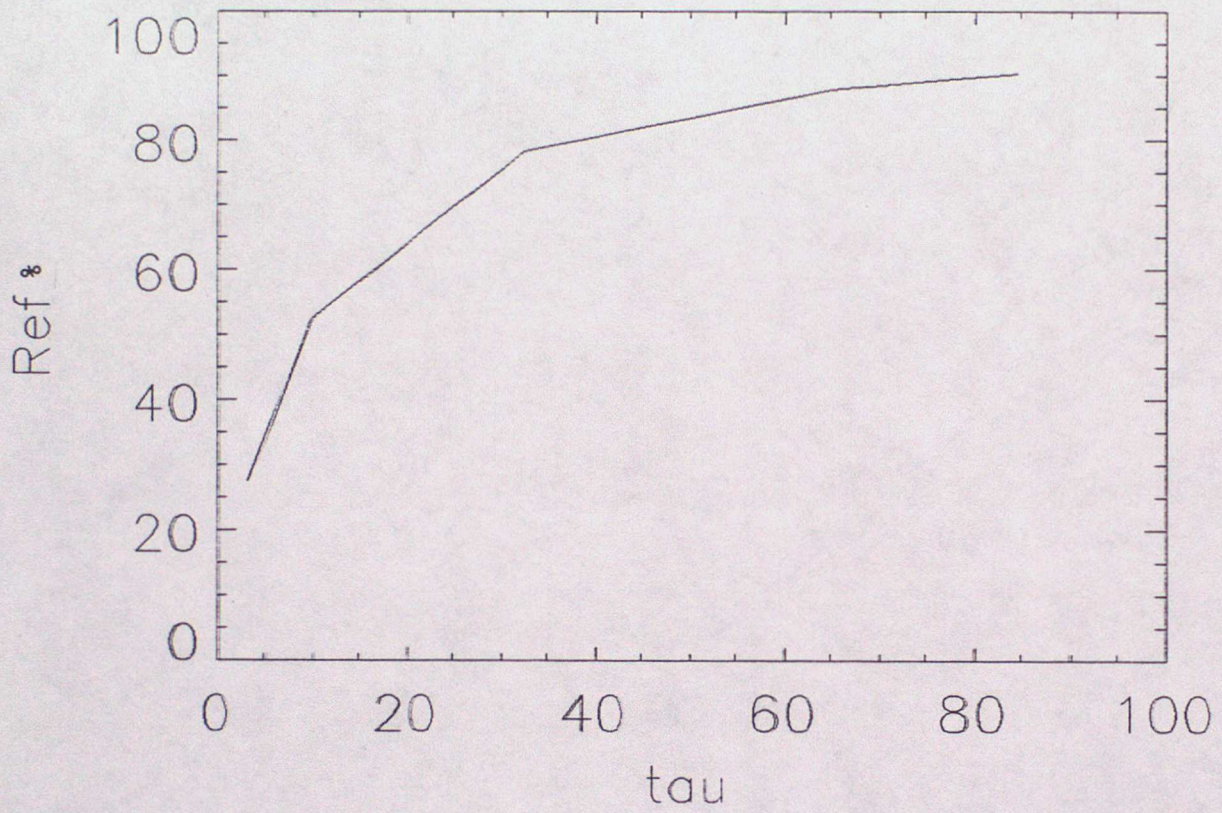


Figure 18. sensitivity of reflectance on optical depth at 0.7 microns for a fixed droplet radius.

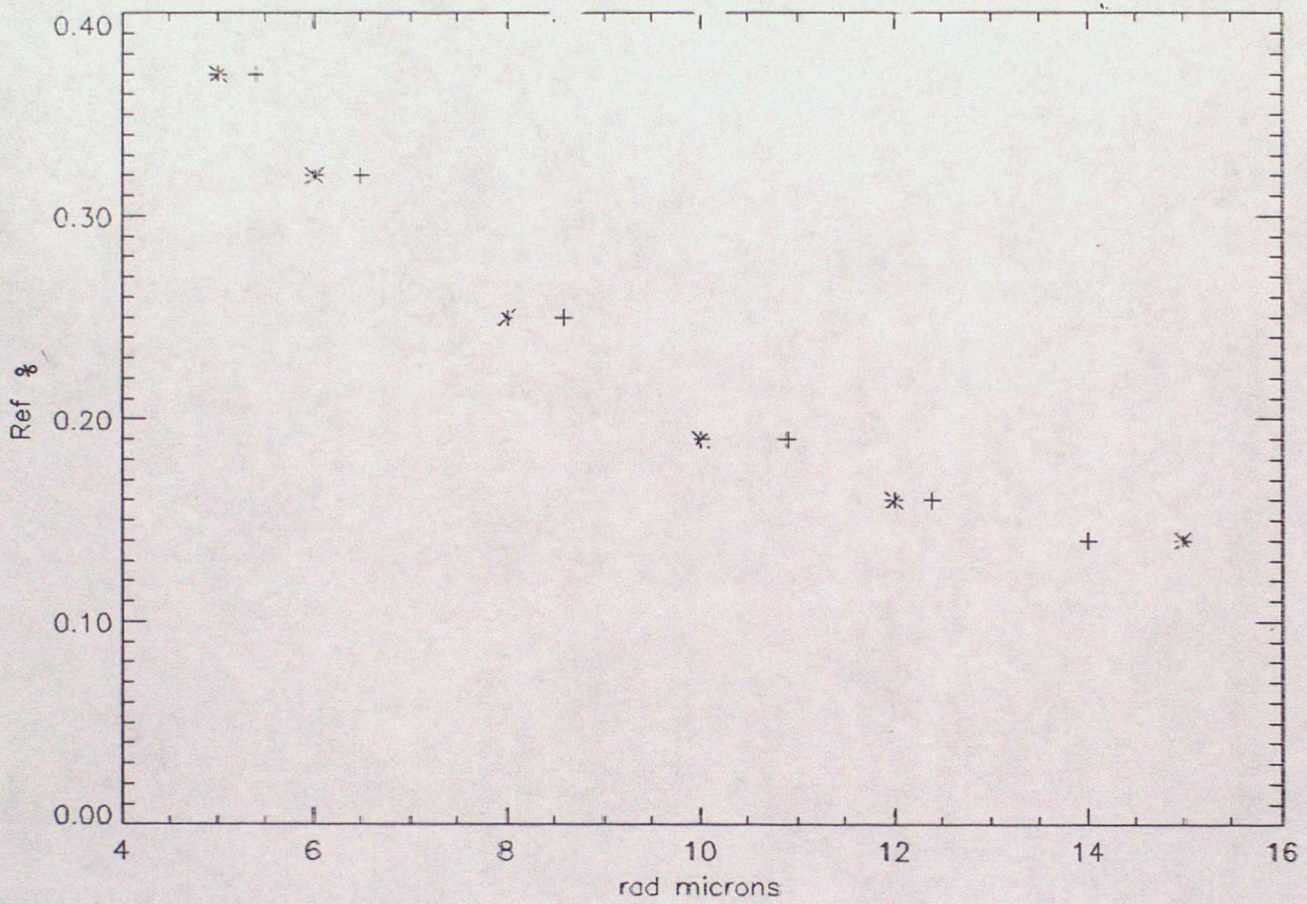
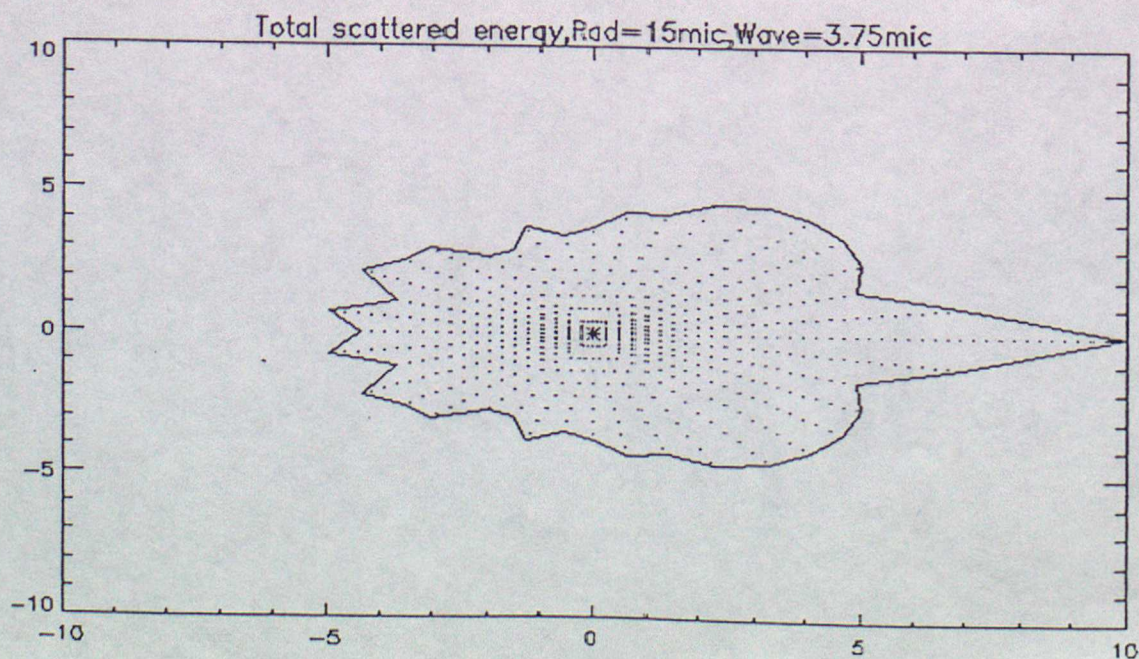
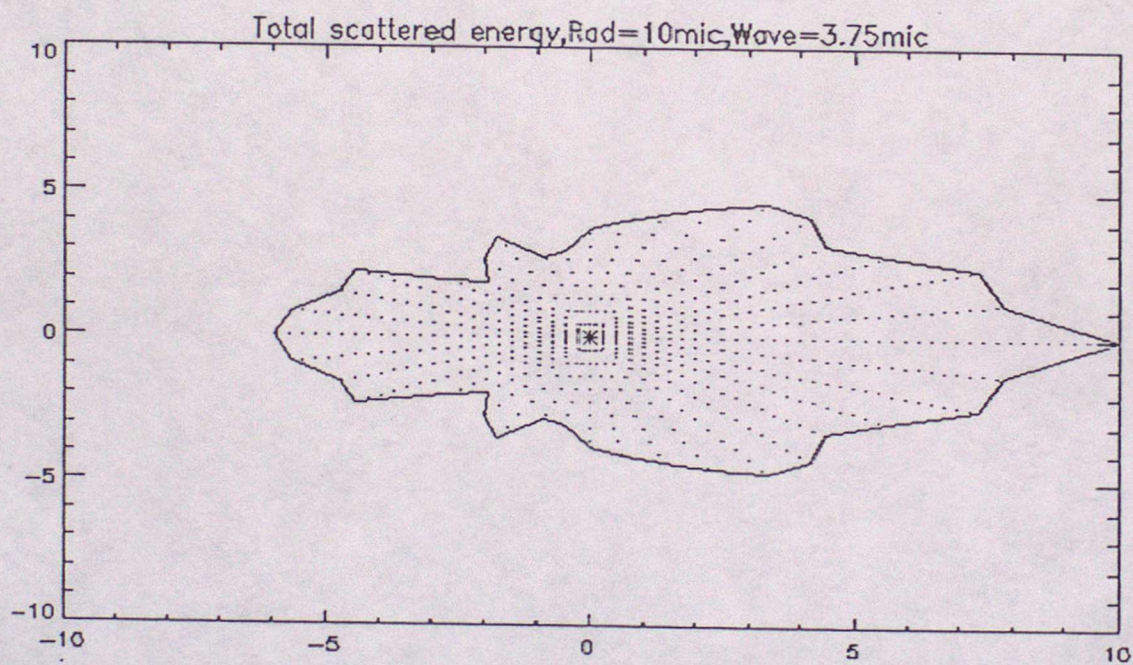
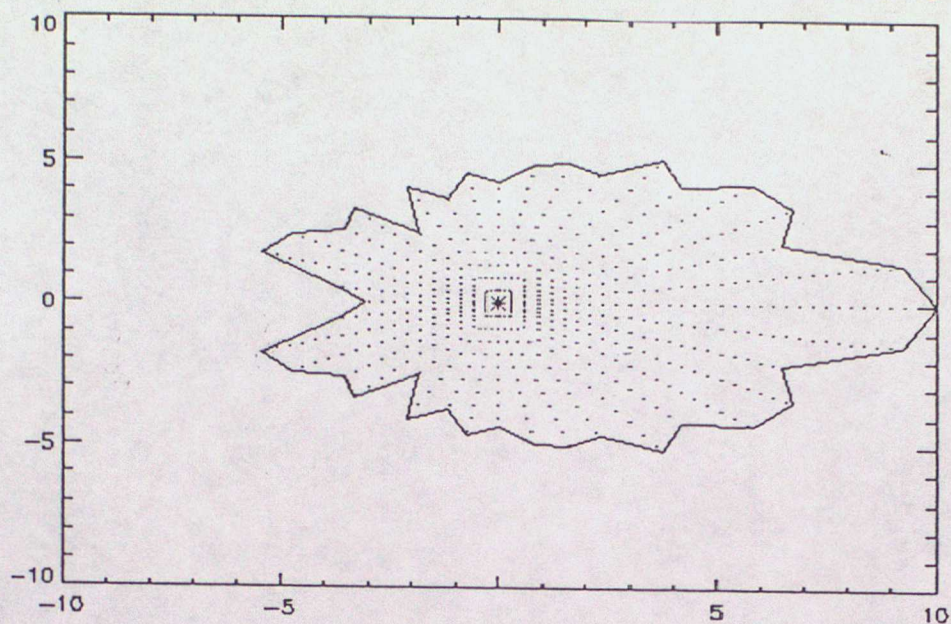


Figure 19. Radius model equation fit to reflectance at 3.75 microns.

+ Radius model equation

* Reflectance at a particular radius.

Figure 20. Polar diagrams of log scattered intensity



SHORT RANGE FORECASTING DIVISION SCIENTIFIC PAPERS

This is a new series to be known as Short Range Forecasting Division Scientific Papers . These will be papers from all three sections of the Short Range Forecasting Research Division i.e. Data Assimilation Research (DA), Numerical Modelling Research (NM), and Observations and Satellite Applications (OB) the latter being formerly known as Nowcasting (NS). This series succeeds the series of Short Range Forecasting Research /Met O 11 Scientific Notes.

1. **THE UNIFIED FORECAST /CLIMATE MODEL .**
M.J.P. Cullen
September 1991

2. **Preparation for the use of Doppler wind lidar information
in meteorological data assimilation systems**
A.C. Lorenc, R.J. Graham, I. Dharssi, B. Macpherson,
N.B. Ingleby, R.W. Lunnon
February 1992

3. **Current developments in very short range weather forecasting.**
B.J. Conway
March 1992

4. **DIAGNOSIS OF VISIBILITY IN THE UK MET OFFICE MESOSCALE MODEL
AND THE USE OF A VISIBILITY ANALYSIS TO CONSTRAIN INITIAL
CONDITIONS**
S.P. Ballard, B.J. Wright, B.W. Golding
April 1992

5. **Radiative Properties of Water and Ice Clouds at Wavelengths
Appropriate to the HIRS Instrument**
A.J. Baran and P.D. Watts
2nd June 1992